2.4. RNA extraction and quantitative RT-PCR analysis

Total cellular RNA (2×10^5 cells/well, 6-well plates) was isolated using TRIzol reagent (Invitrogen, Carlsbad, CA, USA) according to the manufacturer's instruction and purified total RNA using RNeasy Mini Kit (QIAGEN KK, Tokyo, Japan). cDNA synthesis was performed using High Capacity cDNA Reverse Transcription Kit (Applied Biosystems, Foster City, CA, USA), according to the manufacturer's protocol. The PCR was run in microtubes in a volume of 20 μl. The reaction mixture contained 1.0 μl of cDNA, 10 μl of Power SYBR Green PCR Master Mix (Applied Biosystems, Foster City, CA, USA), and 10 pmol of each pair of oligonucleotide primers. The primer sequences were: HMGB1; 5′-ACCCAGATGCTT-CAGTCAAC-3′ (sense), 5′-GGCGATACTCAGAGCAGAAG-3′ (antisense), RAGE; 5′-TCCAGGATGAGGGGATTTTC-3′ (sense), 5′-CCAAGTGCCAGCTAAGAGTC-3′ (antisense). The PCR programme was as follows: initial melting at 95 °C for 10 min and 40 cycles of 30 s at 95 °C, 60 s at 60 °C, 60 s at 72 °C. The quantitation of HMGB1 and RAGE mRNA relative to an internal control, β-actin, was performed.

2.5. Enzyme-linked immunosorbent assay (ELISA)

ELISA was performed for measurement of HMGB1 concentrations in cell culture media by human gingival cells. We have used similar condition (2×10^5 cells/well in 6-well plates) in both RNA (quantitative RT-PCR analysis) and protein (ELISA) experiments. The assay was performed according to the provider's (SHINO-TEST Corporation, Kanagawa, Japan) instructions with triplicate. The experiment was repeated twice.

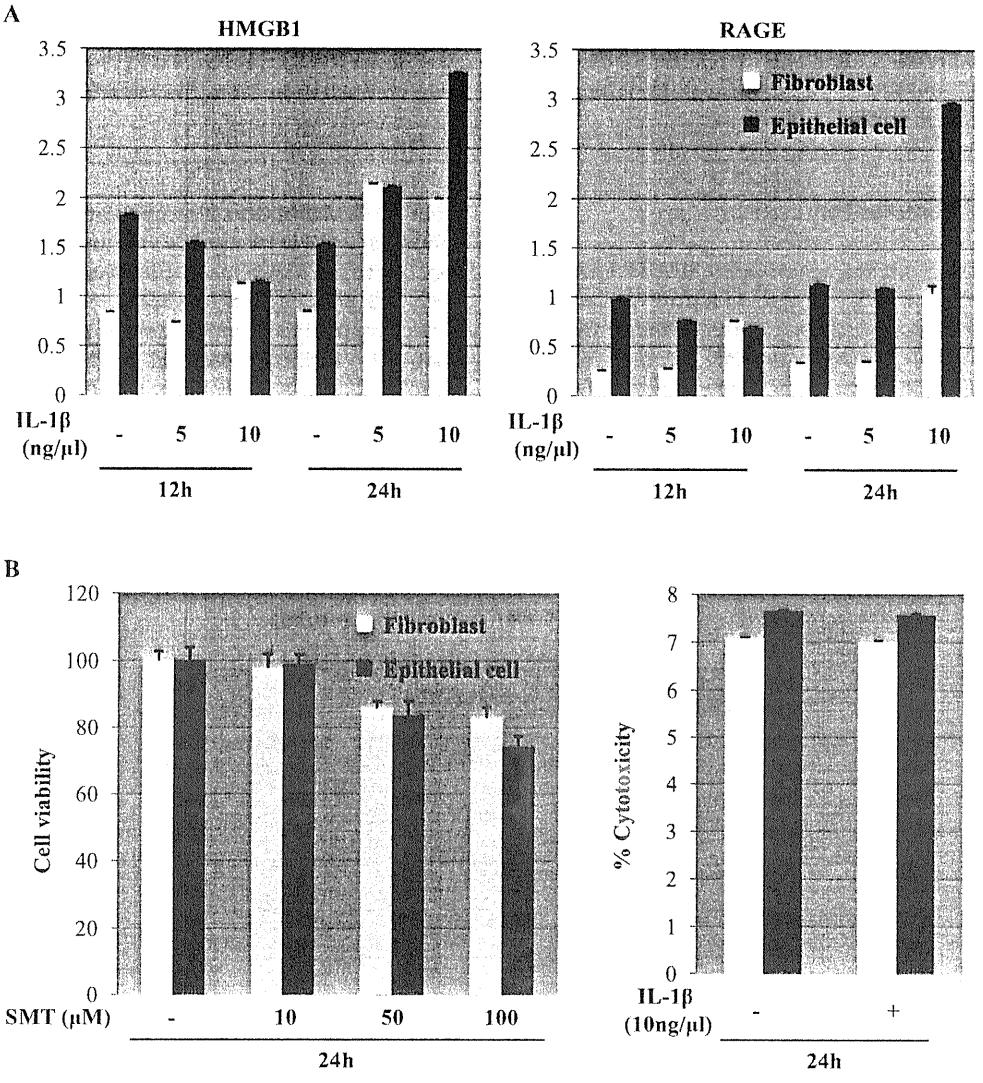

Fig. 1 – Effect of IL-1β in gingival epithelial and fibroblast cell in a concentration-dependant assay and effect of SMT on cell proliferation. (A) Gingival epithelial and fibroblast cells (2×10^5) were exposed to different concentrations of IL-1β for different times and expression of RAGE and HMGB1 was evaluated. (B) MTS assay was performed with different concentrations of SMT for 24 h. LDH activity was measured with IL-1β (10 ng/ml) for 24 h by LDH assay. The experiments were repeated twice in triplicate samples.

Please cite this article in press as: Ito Y, et al. Involvement of HMGB1 and RAGE in IL-1β-induced gingival inflammation. *Archives of Oral Biology* (2011), doi:10.1016/j.archoralbio.2011.08.001

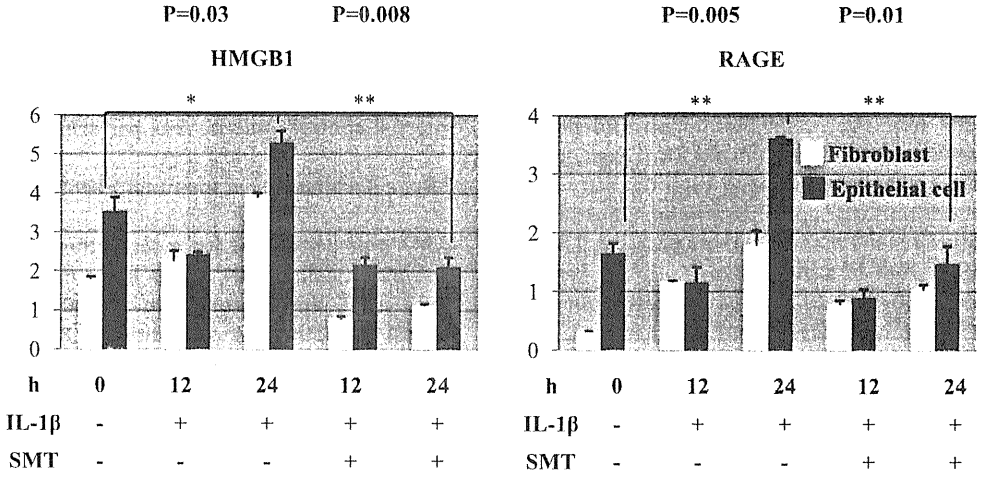

Fig. 2 – Nitric oxide is primarily responsible for the up-regulation observed in gingival cells treated with IL-1β. Gingival epithelial and fibroblast cells (2×10^5) were exposed to IL-1β (10 ng/ml) for different times, and IL-1β increased HMGB1 and RAGE mRNA expression after 24 h by real-time PCR. Pretreatment with an iNOS inhibitor, SMT (10 μM), prevented IL-1β-induced HMGB1 and RAGE release through inhibition of nitric oxide production in cells. The experiments were repeated twice in triplicate samples.

2.6. *Immunohistochemistry*

In total, 27 formalin-fixed, paraffin-embedded specimens (chronic gingivitis $n = 11$, chronic marginal periodontitis $n = 11$, and healthy controls $n = 5$) for examination were obtained from adult patients (14 male, 11 female; mean age ± SD, 56.91 ± 6.56 years). They were subjected to antigen retrieval with pepsin (DAKO, Carpinteria, CA, USA) treatment for 20 min. After blocking endogeneous peroxidase activity with 3% hydrogen peroxide–methanol for 15 min, the specimens were rinsed with phosphate-buffered saline (PBS). Anti-HMGB1 antibody (Upstate biotechnology, Lake Placid, NY, USA; diluted to 0.5%) and anti-RAGE antibody (clone C-20, Santa Cruz Biotechnology, Santa Cruz, CA, USA; diluted to 0.5%) were used as primary antibodies. After a 2-h incubation at room temperature, the specimens were rinsed with PBS and incubated at room temperature for 1 h with secondary antibody conjugated to peroxidase (1:200; anti-goat IgG antibody, Medical & Biological Laboratories, Nagoya, Japan). After rinsing with PBS, all specimens were colour-developed with diaminobenzidine (DAB) solution (DAKO) and counterstained with haematoxylin. The immunostaining of all specimens was performed simultaneously to ensure the same antibody reaction and DAB exposure conditions. Immunoreactivity was evaluated as previously described.[19]

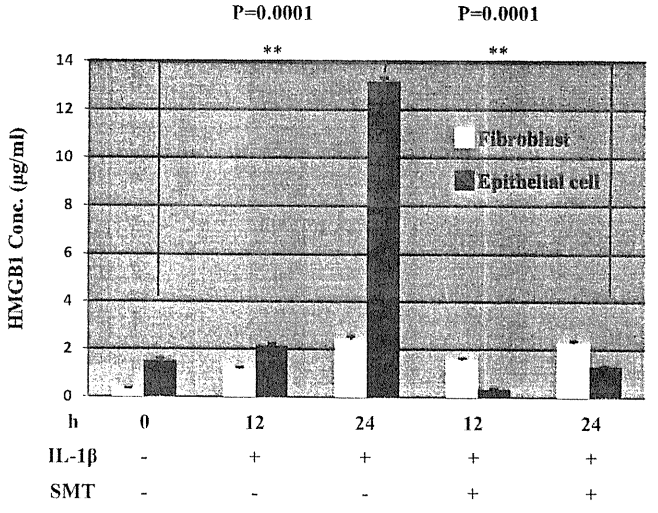

Fig. 3 – HMGB1 is present in cultured gingival cells and released upon IL-1β (10 ng/ml) exposure. Gingival epithelial cells (2×10^5) were treated as indicated overnight, and the levels of HMGB1 in culture supernatants were measured by enzyme-linked immunosorbent assay. The production of HMGB1 was significantly increased. The experiments were repeated twice in triplicate samples.

Please cite this article in press as: Ito Y, et al. Involvement of HMGB1 and RAGE in IL-1β-induced gingival inflammation. *Archives of Oral Biology* (2011), doi:10.1016/j.archoralbio.2011.08.001

2.7. Statistical analyses

Significant differences were analysed by Fisher's exact test. $P < 0.05$ was considered to be statistically significant and $P < 0.01$ highly significant.

3. Results

3.1. IL-1β stimulates HMGB1 and RAGE in a nitric oxide-dependent manner

To understand whether inflammatory gingival activation alters the expression levels of HMGB1 and RAGE, cultures of gingival epithelial and fibroblast cells were exposed to IL-1β for different times, and HMGB1 and RAGE expression was evaluated by real-time PCR. The concentration of IL-1β (10 ng/ml) was adopted from the preliminary study (Fig. 1A). A preliminary screening was done to obtain the optimal concentration of SMT using MTS assay and LDH cytotoxicity in IL-1β-treated cells (Fig. 1B). In line with the cytokine functions of HMGB1, the data demonstrates that IL-1β increased HMGB1 and RAGE expression after 24 h exposure (Fig. 2). IL-1β-induced HMGB1 and RAGE expression was prevented by iNOS inhibitor, SMT (Fig. 2), indicating that nitric oxide is primarily responsible for the up-regulation observed in gingival cells treated with IL-1β.

3.2. HMGB1 is present in cultured gingival cells and released upon IL-1β exposure

To determine whether HMGB1 isolated from IL-1β-exposed cells acquired pro-inflammatory activity, we performed ELISA with conditioned media from gingival epithelial cells cultured with IL-1β. As shown in Fig. 3, HMGB1 concentration was higher in IL-1β-exposed cells, but not with HMGB1 isolated from cells-induced in media lacking IL-1β.

3.3. HMGB1 and RAGE appeared highly expressed in patients with oral inflammation

RAGE expression in normal human gingiva was present predominantly in the granular and spinous layers of epithelial cells, but parabasal cell staining was occasionally present (Fig. 4G). HMGB1 expression was present predominantly in the basal layer of epithelial cells (Fig. 4D). Staining for HMGB1 and RAGE was observed in both epithelial and stromal cells in tissue biopsy samples from all subjects examined. However, clearly increased staining for HMGB1 and RAGE was observed in samples from patients with chronic gingivitis (8 of 11; 72%) (Fig. 4E and H). Similar expression levels and cellular distribution of HMGB1 and RAGE were detected in chronic periodontitis (4 of 11; 36%) (Fig. 4F and I). Inflammatory tissues showed consistently stronger staining, both in its intensity and extent for HMGB1 expression compared with the control.

4. Discussion

HMGB1 is a potent inducer of several pro-inflammatory cytokines. One of these cytokines, IL-1β, is considered a crucial mediator in the pathogenesis of destructive arthritis along with TNFα.[20] Mice deficient for IL-1 receptor did not develop arthritis upon intraarticular administration of HMGB1.[21] IL-1β was bound to HMGB1 isolated from cells cultured with this cytokine, and addition of anti-IL-1β antibodies or the IL-1 receptor antagonist to cell cultures blocked the pro-inflammatory activity of HMGB1[22] further suggesting that the pro-inflammatory action of HMGB1 is likely to be mediated by IL-1β activation. The association of HMGB1 with IL-1β enhanced the pro-inflammatory properties of IL-1β, as cellular activation induced by the HMGB1-IL-1β complex was significantly greater than that found with equivalent amounts of IL-1β alone. These results showed that HMGB1 itself has only minimal pro-inflammatory properties, but it acquires much greater activity through its role as a carrier protein for cytokines or other mediators capable of inducing cell activation. We suggest that HMGB1-triggered oral inflammatory diseases are probably mediated by IL-1β activation.

To provide biochemical evidence in support of IL-1β-induced gingival inflammation, the effects of this cytokine on the release of HMGB1 from epithelial and fibroblast cells was examined. We have confirmed that the cells were alive in culture (Fig. 1B) and HMGB1 was actively released or secreted, but not passively released from necrotic or damaged cells. We showed that IL-1β stimulates HMGB1 release from epithelial cells in a nitric oxide-dependent manner. This effect seemed to be relevant, because the infiltration of RAGE-expressing cells around iNOS-producing cells was observed in the tissue injury associated with periapical periodontitis in a previous study.[23] Our findings suggest that IL-1β-induced HMGB1 release is mediated, at least in part, by nitric oxide, a conclusion further supported by the ability of nitric oxide to directly stimulate HMGB1 release by gingival cells.

Several studies indicated thatHMGB1 could interact with multiple receptors, including RAGE, Toll-like receptor 2 (TLR2), TLR4, and, most recently, TLR9.[24–28] RAGE has some biological characteristics that suggest it may play a pivotal role in the pathogenesis of periodontal disease. It is a tissue receptor, associated with pro-inflammatory response and is expressed differentially in an increased amount with aging.[29] As an important co-factor, increased expression of receptors for adhesion molecules was found on endothelial cells of diabetic patients[30] and these molecules were also associated with severity of periodontal disease.[31] Development of chronic periodontitis could be influenced by polymorphism of the RAGE gene.[32] Increased deposition of AGEs was reported in the gingival of diabetic mice inoculated with *P. gingivalis*.[33] Periodontal disease was also arrested by administration of sRAGE in a murine model.[11,12] RAGE and NF-κB were positively correlated in periapical inflammation.[34] HMGB1 is involved in excessive inflammation regulated by the TNF-α/p38MAPK pathway.[7] Findings presented in this report indicate that RAGE is a major functional receptor mediating the pro-inflammatory effects of HMGB1 in gingival inflammation and activation of RAGE by ligands in a variety of cell types and tissues may play a role in oral systemic associations.

The present study, which to our knowledge is the first to suggest a role for HMGB1/RAGE/iNOS signalling on epithelial cells of human gingiva with periodontal diseases, showed that

Please cite this article in press as: Ito Y, et al. Involvement of HMGB1 and RAGE in IL-1β-induced gingival inflammation. *Archives of Oral Biology* (2011), doi:10.1016/j.archoralbio.2011.08.001

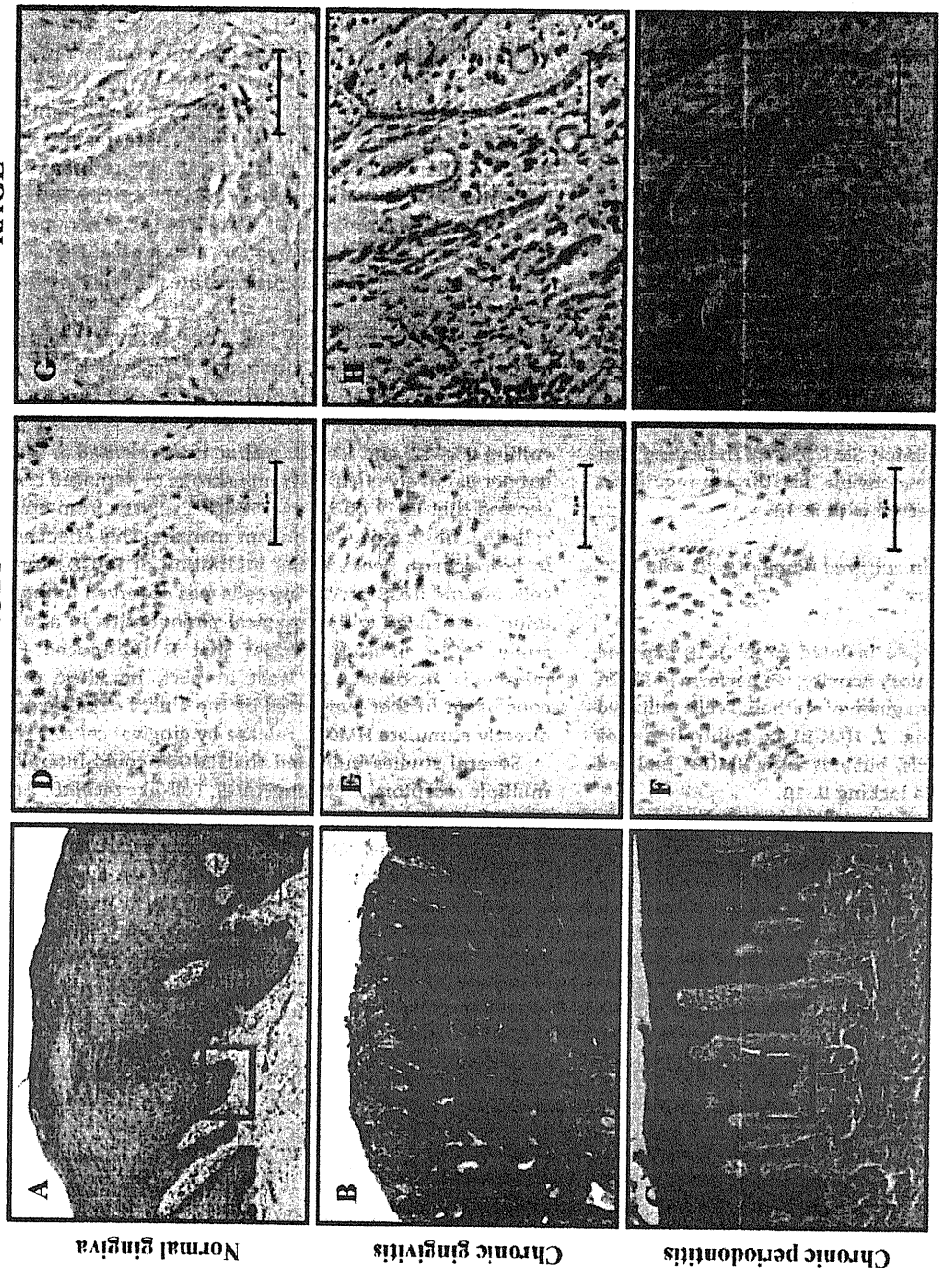

Fig. 4 – HMGB1 and RAGE appeared highly expressed in patients with oral inflammation. Staining for HMGB1 and RAGE in both epithelial and stromal cells from patients with oral inflammatory diseases were increased in comparison with healthy controls. H–E staining: Scale bar = 100 μm; HMGB1 and RAGE staining: Scale bar = 50 μm.

Please cite this article in press as: Ito Y, et al. Involvement of HMGB1 and RAGE in IL-1β-induced gingival inflammation. *Archives of Oral Biology* (2011), doi:10.1016/j.archoralbio.2011.08.001

HMGB1 protein is highly expressed in patients with oral inflammation. Considering the significant influx of macrophage at the site of the local inflammation, their ability to produce a range of tissue-damaging mediators including nitric oxide, and that HMGB1 is released by epithelial cells, we postulate that HMGB1 is a key mediator of chronic inflammation and will be an important therapeutic target in chronic diseases.

In summary, we demonstrated that (1) Human gingival inflammatory epithelial and fibroblast cells constitutively express HMGB1 and RAGE-specific mRNA, (2) IL-1β modulates the expression of HMGB1 and RAGE in human gingival cells and promotes HMGB1 production in human gingival epithelial cells in a nitric oxide-dependent manner, (3) HMGB1 and RAGE are abundantly expressed in gingiva and promptly released during gingival inflammation. Thus, our results may outline a mechanistic explanation for the relationship between chronic inflammation and gingival cell via HMGB1/RAGE/iNOS signalling pathway.

Acknowledgment

This work was supported by Grants-in-Aid from the Ministry of Education, Culture, Sports, Science and Technology of Japan.

Funding: None.

Competing interests: None declared.

Ethical approval: Not required.

Conflict of interests

The authors have no conflicts of interest to declare.

REFERENCES

1. Schilling JD, Mulvey MA, Vincent CD, Lorenz RG, Hultgren SJ. Bacterial invasion augments epithelial cytokine responses to *Escherichia coli* through a lipopolysaccharide-dependent mechanism. *J Immunol* 2001;**166**(2):1148–55.
2. Kokkola R, Sundberg E, Ulfgren AK, Palmblad K, Li J, Wang H, et al. High mobility group box chromosomal protein 1: a novel proinflammatory mediator in synovitis. *Arthritis Rheum* 2002;**46**(10):2598–603.
3. Scaffidi P, Misteli T, Bianchi ME. Release of chromatin protein HMGB1 by necrotic cells triggers inflammation. *Nature* 2002;**418**(6894):191–5.
4. Gardella S, Andrei C, Ferrera D, Lotti LV, Torrisi MR, Bianchi ME, et al. The nuclear protein HMGB1 is secreted by monocytes via a non-classical, vesicle-mediated secretory pathway. *EMBO Rep* 2002;**3**(10):995–1001.
5. Erlandsson Harris H, Andersson U. Mini-review: the nuclear protein HMGB1 as a proinflammatory mediator. *Eur J Immunol* 2004;**34**(10):1503–12.
6. Wang H, Bloom O, Zhang M, Vishnubhakat JM, Ombrellino M, Che J, et al. HMG-1 as a late mediator of endotoxin lethality in mice. *Science* 1999;**285**(5425):248–51.
7. Morimoto Y, Kawahara KI, Tancharoen S, Kikuchi K, Matsuyama T, Hashiguchi T, et al. Tumor necrosis factor-alpha stimulates gingival epithelial cells to release high mobility-group box 1. *J Periodontal Res* 2008;**43**(1):76–83.
8. Thomas HE, Darwiche R, Corbett JA, Kay TW. Interleukin-1 plus gamma-interferon-induced pancreatic beta-cell dysfunction is mediated by beta-cell nitric oxide production. *Diabetes* 2002;**51**(2):311–6.
9. Sakurai H, Kohsaka H, Liu MF, Higashiyama H, Hirata Y, Kanno K, et al. Nitric oxide production and inducible nitric oxide synthase expression in inflammatory arthritides. *J Clin Invest* 1995;**96**(5):2357–63.
10. Sappington PL, Yang R, Yang H, Tracey KJ, Delude RL, Fink MP. HMGB1 B box increases the permeability of Caco-2 enterocytic monolayers and impairs intestinal barrier function in mice. *Gastroenterology* 2002;**123**(3):790–802.
11. Katz J, Bhattacharyya I, Farkhondeh-Kish F, Perez FM, Caudle RM, Heft MW. Expression of the receptor of advanced glycation end products in gingival tissues of type 2 diabetes patients with chronic periodontal disease: a study utilizing immunohistochemistry and RT-PCR. *J Clin Periodontol* 2005;**32**(1):40–4.
12. Katz J, Yoon TY, Mao S, Lamont RJ, Caudle RM. Expression of the receptor of advanced glycation end products in the gingival tissue of smokers with generalized periodontal disease and after nornicotine induction in primary gingival epithelial cells. *J Periodontol* 2007;**78**(4):736–41.
13. Katz J, Caudle RM, Bhattacharyya I, Stewart CM, Cohen DM. Receptor for advanced glycation end product (RAGE) upregulation in human gingival fibroblasts incubated with nornicotine. *J Periodontol* 2005;**76**(7):1171–4.
14. Sasahira T, Kirita T, Bhawal UK, Yamamoto K, Ohmori H, Fujii K, et al. Significance of expression of receptor for advanced glycation end product (RAGE) in recurrence of human oral squamous cell carcinoma. *Histopathology* 2007;**51**(2):166–72.
15. Bhawal UK, Ozaki Y, Nishimura M, Sugiyama M, Sasahira T, Nomura Y, et al. Association of expression of receptors for advanced glycation end-products (RAGE) and invasive and metastatic activity of oral squamous cell carcinoma. *Oncology* 2005;**69**(3):246–55.
16. Kuniyasu H, Sasaki T, Sasahira T, Ohmori H, Takahashi T. Depletion of tumor-infiltrating macrophages is associated with amphoterin expression in colon cancer. *Pathobiology* 2004;**71**(3):129–36.
17. Kuniyasu H, Yano S, Sasaki T, Sasahira T, Sone S, Ohmori H. Colon cancer cell-derived high mobility group 1/amphoterin induces growth inhibition and apoptosis in macrophages. *Am J Pathol* 2005;**166**(3):751–60.
18. Yuspa SH, Harris CC. Altered differentiation of mouse epidermal cells treated with retinyl acetate *in vitro*. *Exp Cell Res* 1974;**86**(1):95–105.
19. Sasahira T, Kirita T, Oue N, Bhawal UK, Yamamoto K, Fujii K, et al. High mobility group box-1-inducible melanoma inhibitory activity is associated with nodal metastasis and lymphangiogenesis in oral squamous cell carcinoma. *Cancer Sci* 2008;**99**(9):1806–12.
20. Andersson U, Wang H, Palmblad K, Aveberger AC, Bloom O, Erlandsson-Harris H, et al. High mobility group 1 protein (HMG-1) stimulates proinflammatory cytokine synthesis in human monocytes. *J Exp Med* 2000;**192**(4):565–70.
21. Pullerits R, Jonsson IM, Verdrengh M, Bokarewa M, Andersson U, Erlandsson-Harris H, et al. High mobility group box chromosomal protein 1, a DNA binding cytokine, induces arthritis. *Arthritis Rheum* 2003;**48**(6):1693–700.
22. Sha Y, Zmijewski J, Xu Z, Abraham E. HMGB1 develops enhanced pro-inflammatory activity by binding to cytokines. *J Immunol* 2008;**180**(4):2531–7.
23. Hama S, Takeichi O, Saito I, Ito K. Involvement of inducible nitric oxide synthase and receptor for advanced glycation

Please cite this article in press as: Ito Y, et al. Involvement of HMGB1 and RAGE in IL-1β-induced gingival inflammation. *Archives of Oral Biology* (2011), doi:10.1016/j.archoralbio.2011.08.001

end products in periapical granulomas. *J Endod* 2007;**33**(2):137–41.
24. Park JS, Svetkauskaite D, He Q, Kim JY, Strassheim D, Ishizaka A, et al. Involvement of Toll-like receptors 2 and 4 in cellular activation by high mobility group box 1 protein. *J Biol Chem* 2004;**279**(9):7370–7.
25. Tian J, Avalos AM, Mao SY, Chen B, Senthil K, Wu H, et al. Toll-like receptor 9-dependent activation by DNA-containing immune complexes is mediated by HMGB1 and RAGE. *Nat Immunol* 2007;**8**(5):487–96.
26. Park JS, Gamboni-Robertson F, He Q, Svetkauskaite D, Kim JY, Strassheim D, et al. High mobility group box 1 protein interacts with multiple Toll-like receptors. *Am J Physiol Cell Physiol* 2006;**290**(3):917–24.
27. Yu M, Wang H, Ding A, Golenbock DT, Latz E, Czura CJ, et al. HMGB1 signals through toll-like receptor (TLR) 4 and TLR2. *Shock* 2006;**26**(2):174–9.
28. Fan J, Li Y, Levy RM, Fan JJ, Hackam DJ, Vodovotz Y, et al. Hemorrhagic shock induces NAD(P)H oxidase activation in neutrophils: role of HMGB1-TLR4 signaling. *J Immunol* 2007;**178**(10):6573–80.
29. Stern DM, Yan SD, Yan SF, Schmidt AM. Receptor for advanced glycation end products (RAGE) and the complications in diabetes. *Ageing Res Rev* 2002;**1**(1):1–15.
30. Schmidt AM, Hori O, Chen JX, Li JF, Crandall J, Zhang J, et al. Advanced glycation end products interacting with their endothelial receptor induce expression of vascular cell adhesion molecule-1 (VCAM-1) in cultured human endothelial cells and in mice. A potential mechanism for the accelerated vasculopathy of diabetes. *J Clin Invest* 1995;**96**(3):1395–403.
31. Joe BH, Borke JL, Keskintepe M, Hanes PJ, Mailhot JM, Singh BB. Interleukin-1 beta regulation of adhesion molecules on human gingival and periodontal ligament fibroblasts. *J Periodontol* 2001;**72**(7):865–70.
32. Holla LI, Kankova K, Fassmann A, Buckova D, Halabala T, Znojil V, et al. Distribution of the receptor for advanced glycation end products gene polymorphisms in patients with chronic periodontitis: a preliminary study. *J Periodontol* 2001;**72**(12):1742–6.
33. Lalla E, Lamster IB, Feit M, Huang L, Spessot A, Qu W, et al. Blockade of RAGE suppresses periodontitis-associated bone loss in diabetic mice. *J Clin Invest* 2000;**105**(8):1117–24.
34. Crabtree M, Pileggi R, Bhattacharyya I, Caudle R, Perez F, Riley J, et al. RAGE mRNA expression and its correlation with nuclear factor kappa beta mRNA expression in inflamed human periradicular tissues. *J Endod* 2008;**34**(6):689–92.

Please cite this article in press as: Ito Y, et al. Involvement of HMGB1 and RAGE in IL-1β-induced gingival inflammation. *Archives of Oral Biology* (2011), doi:10.1016/j.archoralbio.2011.08.001

Profiling of dental plaque microflora on root caries lesions and the protein-denaturing activity of these bacteria

KAZUHIRO HASHIMOTO, DDS, PHD, TAKUICHI SATO, DDS, PHD, HIDETOSHI SHIMAUCHI, DDS, PHD & NOBUHIRO TAKAHASHI, DDS, PHD

ABSTRACT: **Purpose:** To profile plaque microflora on root-caries lesions, and to examine the protein-denaturing activity as a pilot study. **Methods:** Six subjects with root-caries were investigated. Plaque samples on root caries lesions (R), as well as from healthy supragingival sites (S) and periodontal pockets (≥5 mm) (P) were collected and cultured anaerobically on blood agar plates. The isolated bacteria were identified by 16S rRNA sequencing analysis, and examined for the protein-denaturing activity using the skim-milk plates and the SDS-PAGE, and for the acidogenicity using the FAB broth containing 1% glucose. **Results:** *Propionibacterium*, *Actinomyces*, *Streptococcus*, *Lactobacillus* and *Bifidobacterium* were predominant in R, while *Actinomyces*, *Streptococcus*, *Veillonella* and *Capnocytophaga* in S, and *Actinomyces*, *Prevotella*, *Actinobaculum*, *Streptococcus*, *Olsenella* and *Eubacterium* were predominant in P. Proteolytic bacteria comprised 40%, 26% and 57% of microflora in R, S and P, respectively. The skim-milk plates distinguished between protein-degrading and protein-coagulating bacteria, which comprised 7 and 33%, 0 and 26%, and 17 and 40% of microflora, in R, S and P, respectively. The SDS-PAGE analysis revealed that protein-degrading isolates were capable of degrading collagen molecules. Furthermore, the final culture pHs of protein-degrading and -coagulating bacteria were 5.0-5.4 and 3.8-3.9, respectively. The latter pH was low enough to denature proteins in skim milk. The microbial composition of R was distinct from those of S and P. (*Am J Dent* 2011;24:295-299).

CLINICAL SIGNIFICANCE: Cohabitation of coagulating- and degrading-bacteria in R suggested that in the process of root surface caries the former bacteria demineralize hydroxyapatite and denature proteins of root dentin/cementum, and subsequently the latter bacteria degrade denatured proteins.

✉: Dr. Takuichi Sato, Division of Oral Ecology and Biochemistry, Tohoku University Graduate School of Dentistry, Sendai 980-8575, Japan. E-✉: tak@m.tohoku.ac.jp

Introduction

Root caries is a destruction of root, cementum, or cervical area of the tooth of generally elderly people, and is thought to be initiated by decalcification by bacterial acids of plaque formed on root surface, resulting from gingival recession due to periodontitis.[1] The composition of plaque microflora on root caries was more diverse than that on enamel caries, and various bacteria other than *Streptococcus* and *Lactobacillus* may be involved in the onset of caries.[2-4] In addition, degradation of dentin proteins is thought to be related to initiation and progression of root caries, since cementum and dentin of the root surface consist of not only calcium-phosphate but also the proteins such as collagen.[5] Previous studies suggested the involvement of host-derived proteases such as collagenase[6-9] and matrix metalloproteases[10,11] in dentin caries. In addition, it is possible that protein-degrading bacteria are associated with dentin caries, due to the effects of collagenase from *Clostridium* on dentin root demineralization.[12]

Therefore, this study profiled the plaque microflora on root caries lesions using molecular biological techniques, and compared the protein-denaturing activity of plaque bacteria on root caries lesions with those of supragingival and subgingival plaque bacteria, in order to evaluate the relationship between root caries and plaque bacteria.

Materials and Methods

Subjects - Six subjects (two females and four males, age; 48-73 years; mean age 65.5 years) with root caries, who visited the Division of Periodontology and Endodontology, Tohoku University Hospital, Sendai, Japan, were randomly selected for this study. Subjects were free of systemic diseases, received no antibiotics for 3 months and no periodontal treatment for 2 years preceding the sampling. They had neither genetic disease nor smoking habits. In addition, they had more than 20 teeth and no acute inflammation in the oral cavity. Plaque samples on restorative materials (e.g., metal crowns, metal inlays, resin composites) and on clasp-anchored teeth were excluded. Probing depths were measured in all teeth at six sites per tooth in each subject, and in five subjects (A, B, D, E and F; Table 1), more than 30% probing depths (out of all sites) were found to be deeper than 4 mm (maximum 6 mm), indicating that the five subjects suffered from moderate periodontitis. Informed consent was obtained from each subject. This study was approved by the Research Ethics Committee of Tohoku University Graduate School of Dentistry, Sendai, Japan.

Sampling procedure - After sampling sites were isolated by cotton rolls, plaque samples on root caries lesions and from healthy supragingival sites were collected with respective sterile Gracey curettes (SG1/26 or SG5/66[a]). In addition, probing depths were measured in all teeth at six sites per tooth in each subject, and if they were deeper than 4 mm, each subgingival plaque from the deepest periodontal pocket sites was collected with a periodontal pocket probe (Pcpunc15[a]).

Isolation of bacteria - Samples were transported in screw-capped tubes and were transferred as soon as possible to an anaerobic glove box (Model AZ-Hard[b]) containing 80% N_2, 10%H_2 and 10% CO_2. Each sample was weighed, suspended in sterilized 40 mM potassium phosphate buffer (pH 7.0) at a concentration of 1.0 mg/ml and dispersed with a Teflon homo-

Table 1. Clinical features of subjects and bacterial amounts in this study.

	Plaque on root caries lesion							Supragingival plaque					Subgingival plaque					
Subjects	A	B	C	D	E	F	Mean ± SD	C	D	E	F	Mean ± SD	A	B	D	E	F	Mean ± SD
Age	73	69	73	48	66	70	66.5 ± 9.4	73	48	66	70	64.3 ± 11.2	73	69	48	66	70	65.2 ± 9.9
Gender	M	F	M	M	F	M		M	M	F	M		M	F	M	F	M	
Samples sites of plaque*	33	11	37	33	22	43		43	43	22	33		33	21	26	34	14	
Log (CFU/mg)	7.7	6.8	7.7	7.4	7.2	7.2	7.4 ± 7.3	8.2	7.7	7.2	6.6	7.8 ± 7.9	7.6	6.3	7.3	7.1	6.8	7.2 ± 7.2

* A tooth of sampling site is expressed by the FDI two-digit notation.

genizer. Serial 10-fold dilutions (0.1 ml each, from 10^{-4} to 10^{-6}) were spread onto the surface of CDC anaerobe 5% sheep blood agar[c] plates and incubated in the anaerobic glove box at 37°C for 7 days. All plates, media, buffer solutions and experimental instruments were kept in the anaerobic glove box for at least 24 hours before use. To ensure strictly anaerobic condition in the glove box, reduction of methyl-viologen (-446mV) was carefully checked whenever the experimental procedures were carried out. After the incubation, all colonies from plates having <100 colonies (mean 27.9; range 14-38 colonies) were sub-cultured.

DNA extraction and identification by DNA sequence analysis - Genomic DNA was extracted from each single colony with the InstaGene Matrix Kit[d] according to the manufacturer's instructions.

The 16S rRNA gene sequences were amplified by PCR using universal primers 27F and 1492R and Taq DNA polymerase (Hot Star Taq Master Mix[e]), according to the manufacturer's instructions. The primer sequences were: 27F; 5'-AGA GTT TGA TCM TGG CTC AG-3' and 1492R, 5'-TAC GGY TAC CTT GTT ACG ACT T-3'.[13,14] Amplification proceeded using a PCR Thermal Cycler MP[f] programmed as follows: 15 minutes at 95°C for initial heat activation and 30 cycles of 1 minute at 94°C for denaturation, 1 minute at 55°C for annealing, 1.5 minutes at 72°C for extension, and 10 minutes at 72°C for final extension. PCR products were separated on 1% agarose gels (High Strength Analytical Grade Agarose[d]) in Tris-borate EDTA buffer (100 mM Tris, 90 mM borate, 1 mM EDTA; pH 8.4), stained with ethidium bromide and photographed under UV light, and their sizes (ca. 1466 bp) were confirmed comparing with the molecular size marker (a 100 bp DNA Ladder[g]). The PCR products were purified with illustra GFX PCR DNA and Gel Band Purification Kit,[h] and then sequenced at Hokkaido System Science Co. Ltd.[i] using the BigDye Terminator Cycle Sequencing Kit[j] and an automated DNA sequencer (PRISM-3100[j]). Primer 1492R was used to sequence (at least 700 bp), and the partial 16S rRNA gene sequences were then compared with those from the GenBank database using the BLAST search program through the website of the National Center for Biotechnology Information. Bacterial species were determined by percent sequence similarity (>97%).

Determination of protein-coagulating and protein-degrading activity - To determine protein-denaturing activity, bacterial isolates obtained above were cultured on Fastidious Anaerobe Agar (FAA)[k] plates containing 0.75% skim milk[c] (BD) in the anaerobic glove box at 37°C for 7 days. After the incubation, bacteria forming whitish-coagulating zones around their colonies on the FAA-skim milk plates were termed protein-coagulating bacteria, while those forming clear zones on the plates were termed protein-degrading bacteria.

Determination of acid producing activity - To determine acid producing activity, three protein-degrading strains (*Propionibacterium acnes*, *Actinobaculum* sp. oral clone EL030 and *Prevotella denticola*) and two protein-coagulating strains (*Staphylococcus epidermidis* and *Streptococcus mutans*) isolated from root caries lesions in this study were selected. These representative isolates showed the respective same reaction manners on the FAA-skim milk plates. Each one-loopful bacterial colony was collected from the CDC anaerobe blood agar plates and cultured in 500 µl Fastidious Anaerobe Broth (FAB)[k] Lab M containing 1% glucose in the anaerobic glove box at 37°C for 7 days. After the incubation, each pH value of the culture suspensions was measured with a pH meter (Model HM-30G[l]).

Analysis of protein-coagulating and degrading bacteria by SDS-PAGE - To investigate the protein-coagulating and degrading activities in detail, the collagen incubated with the representative isolates (three protein-degrading strains and two protein-coagulating strains) were analyzed by SDS-PAGE.[d] Each one-loopful bacterial colony was collected from the CDC anaerobe blood agar plates and suspended in 100 µl solution of 50 mM Tris-HCl, 0.2 M NaCl, 1 mM $CaCl_2$ (pH 7.5), as reported previously.[15] Then, 10 µl water-soluble type I collagen[m] (0.01%) was added to each solution. The solutions of both immediately and 6 hours after adding type I collagen were analyzed by SDS-PAGE (Ready Gels J, SDS-PAGE standard Broad[d]) in Tris/Glycine/SDS Buffer (25 mM Tris, 192 mM Glycine, 0.1% SDS; pH 8.3) using the CBB R-250 Stain & Destain Kit.[d]

Data analysis - Tukey-Kramer tests were used to analyze significance. P values of <0.05 were considered statistically significant.

Results

The mean bacterial numbers (logCFU/mg of plaque on root caries lesions, healthy supragingival plaque and subgingival plaque of periodontitis were 7.4 ± 7.3, 7.8 ± 7.9, 7.2 ± 7.2, respectively.

Propionibacterium, *Actinomyces*, *Streptococcus*, *Lactobacillus* and *Bifidobacterium* were predominant in plaque on root caries lesions, while *Actinomyces*, *Streptococcus*, *Veillonella* and *Capnocytophaga* were predominant in healthy supragingival plaque. *Actinomyces*, *Prevotella*, *Actinobaculum*, *Streptococcus*, *Olsenella* and *Eubacterium* were predominant in subgingival plaque of periodontitis (Table 2).

The skim-milk plates distinguished between protein-degrading and protein-coagulating bacteria. The proportions

Table 2. Predominant bacterial genera in plaque on root caries lesion, supragingival plaque and subgingival plaque.

	Plaque on root caries lesion		Supragingival plaque		Subgingival plaque	
	179[a]	(100)[b]	123	(100)	116	(100)
Propionibacterium	50	(27.9)	1	(0.8)	5	(4.3)
Actinomyces	36	(20.1)	54	(43.9)	25	(21.6)
Streptococcus	22	(12.3)	22	(17.9)	9	(7.8)
Lactobacillus	14	(7.8)	2	(1.6)		
Bifidobacterium	11	(6.1)				
Veillonella	10	(5.6)	15	(12.2)	2	(1.7)
Prevotella	9	(5.0)	5	(4.1)	18	(15.5)
Staphylococcus	8	(4.5)			2	(1.7)
Actinobaculum	6	(3.4)			11	(9.5)
Capnocytophaga	4	(2.2)	10	(8.1)	3	(2.6)
Campylobacter	3	(1.7)	6	(4.9)	4	(3.4)
Selenomonas	2	(1.1)	4	(3.3)	4	(3.4)
Eubacterium	1	(0.6)	1	(0.8)	7	(6.0)
Leptotrichia	1	(0.6)			1	(0.9)
Olsenella	1	(0.6)			8	(6.9)
Human oral bacterium AC1	1	(0.6)				
Fusobacterium					3	(2.6)
Peptostreptococcus					3	(2.6)
Dialister					2	(1.7)
Gemella					2	(1.7)
Megashaera					2	(1.7)
Corynbacterium					1	(0.9)
Eikenella			1	(0.8)		
Neisseria					1	(0.9)
Porphyromonas					1	(0.9)
Bacteroides-like sp.					1	(0.9)
Kingella			1	(0.8)		
TM7 Phylum			1	(0.8)		

[a] Number of bacterial strains isolated.
[b] Percentages are given in parentheses.

of protein-degrading and protein-coagulating bacteria in plaque on root caries lesions, healthy supragingival plaque and subgingival plaque of periodontitis were 7 and 33%, 0 and 26%, and 17 and 40% of microflora, respectively. The proportion of protein-denaturing bacteria (protein-coagulating plus protein-degrading bacteria) in subgingival plaque was significantly higher than that of the other two groups (Table 3), and the proportion in root caries was also found to be higher than that of supragingival plaque, although the difference was not statistically significant (Table 3).

Among protein-coagulating bacteria isolated from plaque on root caries lesions, *Actinomyces*, *Streptococcus*, *Lactobacillus* and *Bifidobacterium* were predominant, while *Prevotella*, *Actinobaculum* and *Propionibacterium* were predominant in protein-degrading isolates (Table 4). From supragingival plaque, only protein-coagulating bacteria were isolated and identified mainly as *Actinomyces*, *Streptococcus* and *Prevotella*. In subgingival plaque of periodontitis, protein-coagulating isolates were identified mainly as *Actinomyces* and *Actinobaculum*, while *Prevotella* was predominant in protein-degrading isolates (Table 4).

The final pH of representative protein-degrading bacteria, *P. acnes*, *Actinobaculum* sp. oral clone EL030 and *P. denticola*, were 5.4, 5.0 and 5.3, respectively, while, that of representative protein-coagulating bacteria, *S. mutans* and *S. epidermidis*, were 3.8 and 3.9, respectively. Preliminary experiments showed that the skim milk plates were coagulated at pH 3.5 and 4.0, but not coagulated at pH 4.5 and 5.0.

The SDS-PAGE analysis of collagen degradation by representative protein-degrading bacteria (*P. acnes*, *Actinobaculum* sp. oral clone EL030 and *P. denticola*) showed that the collagen bands (ca. 200 and 130 kDa) were faded out during a 6-hour incubation, and several small peptide bands appeared (ca. 70, 25 and 10 KDa in *P. acnes*, ca. 17 KDa in *Actinobaculum* sp. oral clone EL030, and smear bands in *P. denticola*). On the other hand, representative protein-coagulating bacteria *S. mutans* and *S. epidermidis* did not change the band profiles for 6-hour incubation (Figure).

Table 3. Number and proportion of protein-coagulating and -degrading bacteria in plaque on root caries lesion, supragingival plaque and subgingival plaque.

	Plaque on root caries lesion	Supragingival plaque	Subgingival plaque
Coagulating bacteria[a]	60	32	47
Degrading bacteria[a]	13	0	20
Coagulating bacteria + degrading bacteria[a]	73	32	67
Total bacterial strains isolated	179	123	116
Proportion of coagulating bacteria (%)	33.1[b]	26.2[b]	39.6[b]
Proportion of degrading bacteria (%)	7.2[c]	0.0[c]	17.0[c]
Proportion of coagulating bacteria + degrading bacteria (%)	40.4[d]	26.2[d]	56.6[e]

[a] Number of bacterial strains isolated.
[b] Not significantly different among plaque on root caries lesion, supragingival plaque and subgingival plaque.
[c] Not significantly different among plaque on root caries lesion, supragingival plaque and subgingival plaque.
[d, e] Significantly different ($P < 0.05$) between plaque on root caries lesion and subgingival plaque; and supragingival plaque and subgingival plaque.

Discussion

In this study, *Propionibacterium*, *Actinomyces*, *Streptococcus*, *Lactobacillus* and *Bifidobacterium* were predominant in plaque microflora on root caries lesions (Table 2). *Actinomyces*, *Streptococcus* and *Lactobacillus* were predominant on root caries lesions,[2,16-19] in accordance with this study. *Propionibacterium* and *Bifidobacterium* as well as *Actinomyces*, *Streptococcus* and *Lactobacillus* are reportedly often detected from carious dentin,[20,21] thus suggesting that plaque microflora on root caries lesions is similar to that of carious dentin. Preza *et al*[22] reported, utilizing the cloning and sequencing methods, that *Atopobium*, *Olsenella*, *Propionibacterium* and other bacteria, as well as mutans streptococci, *Lactobacillus* and *Actinomyces*, were detected in plaque on the root caries lesions of the elderly.

In this study, bacteria responding to the skim milk plates were divided into two groups termed the protein-coagulating bacteria that denatured and coagulated proteins in the skim milk, and protein-degrading bacteria that degraded and solubilized the proteins in the skim milk. The total proportion of protein-coagulating and -degrading bacteria in plaque microflora on root caries lesions (40%) was higher than that in healthy supragingival plaque (26%), although the difference was not statistically significant (Table 3).

In addition, the SDS-PAGE analysis revealed that protein-degrading bacteria isolated from plaque on root caries lesions were capable of degrading collagen molecules into small peptides (Figure), suggesting that protein-degrading bacteria such as *Actinobaculum*, *Prevotella* and *Propionibacterium* are involved in root caries formation through collagen degradation. The SDS-PAGE analysis also showed the variety in peptide profile after bacterial degradation of collagen (Figure), indi-

Table 4. Predominant protein-coagulating and degrading bacterial genera in plaque on root caries lesion, supragingival plaque and subgingival plaque.

	Plaque on root caries lesion						Supragingival plaque						Subgingival plaque					
Total isolates	Coagulating 60		Degrading 13		Total 73		Coagulating 32		Degrading 0		Total 32		Coagulating 47		Degrading 20		Total 67	
Actinomyces	20[a]	(27.4)[b]	0	(0.0)	20	(27.4)	13	(40.6)	0	(0.0)	13	(40.6)	19	(28.4)	1	(1.5)	20	(29.9)
Streptococcus	15	(20.5)	0	(0.0)	15	(20.5)	13	(40.6)	0	(0.0)	13	(40.6)	6	(9.1)	0	(0.0)	6	(9.1)
Lactobacillus	9	(12.3)	0	(0.0)	9	(12.3)												
Bifidobacterium	8	(11.0)	0	(0.0)	8	(11.0)												
Actinobaculum	0	(0.0)	6	(8.2)	6	(8.2)							10	(14.9)	0	(0.0)	10	(14.9)
Staphylococcus	6	(8.2)	0	(0.0)	6	(8.2)							1	(1.5)	0	(0.0)	1	(1.5)
Prevotella	1	(1.4)	3	(4.1)	4	(5.5)	4	(12.5)	0	(0.0)	4	(12.5)	5	(7.6)	13	(19.7)	18	(27.3)
Propionibacterium	0	(0.0)	3	(4.1)	3	(4.1)							0	(0.0)	3	(4.5)	3	(4.5)
Selenomonas	1	(1.4)	0	(0.0)	1	(1.4)	1	(3.1)	0	(0.0)	1	(3.1)	1	(1.5)	0	(0.0)	1	(1.5)
Olsenella	0	(0.0)	1	(1.4)	1	(1.4)							0	(0.0)	1	(1.5)	1	(1.5)
Capnocytophaga							1	(3.1)	0	(0.0)	1	(3.1)	2	(3.0)	0	(0.0)	2	(3.0)
Fusobacterium													2	(3.0)	0	(0.0)	2	(3.0)
Neisseria													1	(1.5)	0	(0.0)	1	(1.5)
Peptostreptococcus													0	(0.0)	1	(1.5)	1	(1.5)
Porphyromonas													0	(0.0)	1	(1.5)	1	(1.5)

[a] Number of bacterial strains isolated.
[b] Percentages are given in parentheses.

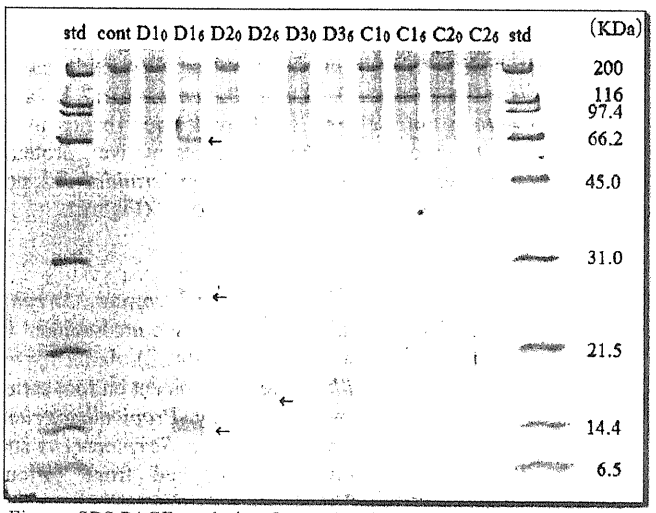

Figure. SDS-PAGE analysis of type I collagen degradation by bacterial strains isolated in this study. cont: Control (only Type I collagen), $D1_0$ and $D1_6$: *Propionibacterium acnes*, $D2_0$ and $D2_6$: *Actinobaculum* sp. oral clone EL030, $D3_0$ and $D3_6$: *Prevotella denticola*, C10 and C16: *Staphylococcus epidermidis*, C20 and C26: *Streptococcus mutans*. $D1_0$, $D2_0$, $D3_0$, $C1_0$, and $C2_0$: Immediately after adding type I collagen; and $D1_6$, $D2_6$, $D3_6$, $C1_6$, and $C2_6$: 6 hours after adding type I collagen. std: Standard (SDS-PAGE Standard Broad).[d] Appeared bands (ca. 70, 25 and 10 KDa in *P. acnes*, and ca. 17 KDa in *Actinobaculum* sp. oral clone EL030) are marked with arrows.

cating the diversity of bacterial collagenases, as reported previously.[23] In contrast, protein-coagulating bacteria did not degrade collagen (Figure), but produced enough organic acids to denature proteins, i.e., alter protein conformation, since they lowered the pH of the medium to approximately 4.0 where the skim milk was found to be coagulated in the skim milk plates. Root collagen is degraded by collagenase after pretreatment of the demineralization by organic acids,[12] and acid-pretreatment of collagen enhances degradation of protein by collagenase.[24] Thus, the coexistence of protein-degrading and protein-coagulating bacteria in root caries lesions suggests the cooperation of these bacteria in the onset and progression of root caries. More specifically, the protein-coagulating bacteria, such as *Actinomyces*, *Streptococcus*, *Lactobacillus* and *Bifidobacterium*, may demineralize the inorganic components and denature organic components including collagen of root cementum and dentin, and then the protein-degrading bacteria, such as *Prevotella*, *Actinobaculum* and *Propionibacterium*, may degrade the denatured proteins, thus resulting in the onset and progression of root caries (Table 4). In the latter process, host-derived proteases including matrix metalloproteases contained in saliva and host tissues also may be involved.[10,11]

The proportion of the protein-coagulating plus protein-degrading bacteria in subgingival plaque (57%) was significantly higher than in plaque on root caries lesions and in supragingival plaque. Particularly, the proportion of the protein-degrading bacteria (17%) was the highest among the three groups (Table 3), supporting the proposal by Grenier & Turgeon[25] that the protein-degrading bacteria may play an important role in the pathogenesis of periodontitis. The mean proportion of protein-degrading bacteria in subgingival plaque (28%, range of 7-65%) in their study was higher than that of the present study (mean 17%, range 0 - 38%). The discrepancy may be due to the probing depths of the study by Grenier & Turgeon[25] (mean 7.3 mm, range 6-10 mm) which were deeper than those of this study (mean 5.3 mm, range 5-6 mm), since the protein-degrading bacteria may be more likely to inhabit the deeper periodontal pockets, where nitrogenic compounds including proteins are abundant and supplied continuously.[26]

Root caries is closely associated with periodontal therapy and often occurs following periodontal therapy.[27] Although the periodontal therapy improves the condition of periodontal tissues and reduces the number of periodontitis-associated bacteria, the exposed root surfaces are often challenged by acids produced from carbohydrates contained in foods, and subsequently the demineralization of the surfaces likely occurs. In addition, it is possible that the organic components in the root surface are denatured at the low pH, and that the denatured organic components are then degraded by the protein-degrading bacteria, as well as host-derived proteases. These processes may result in the initiation of root caries. To verify this proposition, a comprehensive study including analysis on non-collagenous proteins and host-derived pro-

teases (matrix metalloproteases) is required. As the number of plaque samples examined in this study was relatively small, further studies including large-scale studies are clearly required. On the basis of the findings of the present study, the supportive periodontal and maintenance therapy, whose importance has been reported,[28-30] should be performed following the active periodontal therapy.

a. Hu-Friedy, Chicago, IL, USA.
b. Hirasawa, Tokyo, Japan.
c. BD, Franklin Lakes, NJ, USA.
d. Bio-Rad Laboratories, Richmond, CA, USA.
e. Qiagen GmbH, Hilden, Germany.
f. TaKaRa Biomedicals, Ohtsu, Shiga, Japan.
g. Invitrogen Corp., Carlsbad, CA, USA.
h. GE Healthcare, UK Ltd., Buckinghamshire, UK.
i. Hokkaido System Science Co., Ltd., Sapporo, Japan.
j. Applied Biosystem Japan Ltd., Tokyo, Japan.
k. Lab M, Bury, UK.
l. DKK-TOA Co., Tokyo, Japan.
m. FIP, Yamagata, Japan.

Disclosure statement: The authors declared no conflict of interest. This study was supported in part by Grants-in-Aid for Scientific Research (20592220, 22390399, 23592791) from the Ministry of Education, Culture, Sports, Science and Technology, Japan.

Dr. Hashimoto is an Adjunct Instructor, Division of Periodontology and Endodontology, and a former graduate student, Division of Oral Ecology and Biochemistry, Dr. Sato is a Lecturer, Division of Oral Ecology and Biochemistry, Dr. Shimauchi is a Professor, Division of Periodontology and Endodontology. Dr. Takahashi is a Professor, Division of Oral Ecology and Biochemistry, Tohoku University Graduate School of Dentistry, Sendai, Japan.

References

1. Beighton D, Brailsford SR. Plaque microbiology of root caries. In: Newman HN, Wilson M. *Dental plaque revisited.* Cardiff; BioLine, 1999;295-312.
2. Bowden GHW. Microbiology of root surface caries in humans. *J Dent Res* 1990;69:1205-1210.
3. Bowden GHW, Ekstrand J, McNaughton B, Challacombe SJ. The association of selected bacteria with the lesions of root surface caries. *Oral Microbiol Immunol* 1990;5:346-351.
4. Brailsford SR, Shah B, Simons D, Gilbert S, Clark D, Ines I, Adams SE, Allison C, Beighton D. The predominant aciduric microflora of root-caries lesions. *J Dent Res* 2001;80:1828-1833.
5. Steinfort J, Deblauwe BM, Beertsen W. The inorganic components of cementum- and enamel-related dentin in the rat incisor. *J Dent Res* 1990;69:1287-1292.
6. Weill R, Lormee P, Goldberg M, Escaig F. Matrix alteration in rat caries. *Caries Res* 1977;11:95-99.
7. Dayan D, Binderman I, Mechanic GL. A preliminary study of activation of collagenase in carious human dentine matrix. *Arch Oral Biol* 1983;28:185-187.
8. Armstrong WG. A quantitative comparison of the amino acid composition of sound dentine, carious dentine and the collagenase resistant fraction of carious dentine. *Arch Oral Biol* 1961;5:115-124.
9. Dumasa J, Huriona N, Weillb R, Keila B. Collagenase in mineralized tissues of human teeth. *FEBS Lett* 1985;187:51-55.
10. Chaussain-Miller C, Fioretti F, Goldberg M, Menashi S. The role of matrix metalloproteinases (MMPs) in human caries. *J Dent Res* 2006;85:22-32.
11. Tjäderhane L, Larjava H, Sorsa T, Uitto VJ, Larmas M, Salo T. The activation and function of host matrix metalloproteinases in dentin matrix breakdown in caries lesions. *J Dent Res* 1998;77:1622-1629.
12. Kawasaki K, Featherstone JDB. Effects of collagenase on root demineralization. *J Dent Res* 1997;76:588-595.
13. Lane DJ. 16S/23S rRNA sequencing. In: Stackebrandt E, Goodfellow M. *Nucleic acid techniques in bacterial systematics*. Chichester: John Wiley & Sons, 1991;115-175.
14. Marchesi JR, Sato T, Weightman AJ, Martin TA, Fry JC, Hiom SJ, Dymock D, Wade WG. Design and evaluation of useful bacterium-specific PCR primers that amplify genes coding for bacterial 16S rRNA. *Appl Environ Microbiol* 1998;64:795-799.
15. Sorsa T, Ding YL, Ingman T, Salo T, Westerlund U, Haapasalo M, Tschesche H, Konttinen YT. Cellular source, activation and inhibition of dental plaque collagenase. *J Clin Periodontol* 1995;22:709-717.
16. Brown LR, Billings RJ, Kaster AG. Quantitative comparisons of potentially cariogenic microorganisms cultured from noncarious and carious root and coronal tooth surfaces. *Infect Immun* 1986;51:765-770.
17. Ellen RP, Bnting DW, Fillery ED. *Streptococcus mutans* and *Lactobacillus* detection in the assessment of dental root surface caries risk. *J Dent Res* 1985;64:1245-1249.
18. Ellen RP, Banting DW, Fillery ED. Longitudinal microbiological investigation of a hospitalized population of older adults with a high root surface caries risk. *J Dent Res* 1985;64:1377-1381.
19. van Houte J, Lopman J, Kent R. The predominant cultivable flora of sound and carious human root surfaces. *J Dent Res* 1994;73:1727-1734.
20. Hoshino E. Predominant obligate anaerobes in human carious dentin. *J Dent Res* 1985;64:1195-1198.
21. Wade WG, Munson MA, de Lillo A, Weightman AJ. Specificity of the oral microflora in dental caries, endodontics infections and periodontitis. *Int Cong Ser* 2005;1284:150-157.
22. Preza D, Olsen I, Aas JA, Willumsen T, Grinde B, Paster BJ. Bacterial profiles of root caries in elderly patients. *J Clin Microbiol* 2008;46:2015-2021.
23. Bedran-Russo AKB, Yoo KJ, Ema KC, Pashley DH. Mechanical properties of tannic-acid-treated dentin matrix. *J Dent Res* 2009;88:807-811.
24. van Strijp AJ, Klont B, Ten Cate JM. Solubilization of dentin matrix collagen *in situ*. *J Dent Res* 1992;71:1498-1502.
25. Grenier D, Turgeon J. Occurrence and identity of proteolytic bacteria in adult periodontitis. *J Periodont Res* 1994;29:365-370.
26. Takahashi N. Microbial ecosystem in the oral cavity: Metabolic diversity in an ecological niche and its relationship with oral diseases. *Int Cong Ser* 2005;1284:103-112.
27. Boehm TK, Scannapieco FA. The epidemiology, consequences and management of periodontal disease in older adults. *J Am Dent Assoc* 2007;138:26-33.
28. Bizhang M, Chun YHP, Heisrath D, Purucker P, Singh P, Kersten T, Zimmer S. Microbiota of exposed root surfaces after fluoride, chlorhexidine, and periodontal maintenance therapy: A 3-year evaluation. *J Periodontol* 2007;78:1580-1589.
29. Quirynen M, Gizani S, Mongardini C, Declerck D, Vinckier F, van Steenberghe D. The effect of periodontal therapy on the number of cariogenic bacteria in different intra-oral niches. *J Clin Periodontol* 1999;26:322-327.
30. Reiker J, van der Velden U, Barendregt DS, Loos BG. A cross-sectional study into the prevalence of root caries in periodontal maintenance patients. *J Clin Periodontol* 1999;26:26-32.

RESEARCH REPORTS
Biological

N. Takahashi* and J. Washio

Division of Oral Ecology and Biochemistry, Department of Oral Biology, Tohoku University Graduate School of Dentistry, 4-1 Seiryo-machi, Aoba-ku, Sendai 980-8575, Japan; *corresponding author, nobu-t@dent.tohoku.ac.jp

J Dent Res 90(12):1463-1468, 2011

Metabolomic Effects of Xylitol and Fluoride on Plaque Biofilm *in Vivo*

ABSTRACT

Dental caries is initiated by demineralization of the tooth surface through acid production from sugar by plaque biofilm. Fluoride and xylitol have been used worldwide as caries-preventive reagents, based on *in vitro*–proven inhibitory mechanisms on bacterial acid production. We attempted to confirm the inhibitory mechanisms of fluoride and xylitol *in vivo* by performing metabolome analysis on the central carbon metabolism in supragingival plaque using the combination of capillary electrophoresis and a time-of-flight mass spectrometer. Fluoride (225 and 900 ppm F^-) inhibited lactate production from 10% glucose by 34% and 46%, respectively, along with the increase in 3-phosphoglycerate and the decrease in phosphoenolpyruvate in the EMP pathway in supragingival plaque. These results confirmed that fluoride inhibited bacterial enolase in the EMP pathway and subsequently repressed acid production *in vivo*. In contrast, 10% xylitol had no effect on acid production and the metabolome profile in supragingival plaque, although xylitol 5-phosphate was produced. These results suggest that xylitol is not an inhibitor of plaque acid production but rather a non-fermentative sugar alcohol. Metabolome analyses of plaque biofilm can be applied for monitoring the efficacy of dietary components and medicines for plaque biofilm, leading to the development of effective plaque control.

KEY WORDS: metabolome analysis, supragingival plaque, sugar metabolism, fluoride, xylitol, dental caries.

DOI: 10.1177/0022034511423395

Received June 3, 2011; Last revision August 22, 2011; Accepted August 23, 2011

INTRODUCTION

Fluoride and xylitol have been used worldwide as representative caries-preventive reagents. Fluoride inhibits demineralization and promotes remineralization of the tooth surface (ten Cate, 1999; Fejerskov, 2004). Fluoride is also known to inhibit bacterial acid production *in vitro* (Hamilton, 1990; Marquis, 1990; Jenkins, 1999) and plaque acid production *in vivo* (Tatevossian, 1990; Vogel *et al.*, 2002). Competitive inhibition by fluoride of enolase, an enzyme in the Embden-Meyerhof-Parnas pathway (the EMP pathway) extracted from *Streptococcus mutans* and other plaque bacteria (Kaufmann and Bartholmes, 1992; Guha-Chowdhury *et al.*, 1997), suggested that enolase is the target enzyme by fluoride inhibition. The addition of fluoride to a cell suspension of *S. mutans, S. sobrinus*, and *S. sanguinis* results in the intracellular accumulation of 3-phosphoglycerate and 2-phosphoglycerate (enolase substrate) and the decrease of phosphoenolpyruvate (enolase product) in the EMP pathway (Hata *et al.*, 1990; Maehara *et al.*, 2005), confirming the inhibition of enolase by fluoride; however, the inhibitory mechanism of fluoride has not been confirmed in plaque biofilm, consisting of multispecies of bacteria, where they may behave differently compared with *in vitro* behavior.

Xylitol is a non-fermentative sugar alcohol, and thus does not cause dental caries, similar to other sugar alcohols. Xylitol is known to repress acid production from glucose by *S. mutans* through the inhibition of glycolytic enzymes by xylitol 5-phosphate (X5P) produced from xylitol by a constitutive phosphoenolpyruvate:fructose phosphotransferase system (Assev and Rölla, 1984; Trahan *et al.*, 1985; Trahan, 1995; Miyasawa *et al.*, 2003). Further, X5P is dephosphorylated and returned to xylitol, resulting in the formation of a "futile cycle", an energy-wasting cycle, and the subsequent repression of growth of *S. mutans* (Pihlanto-Leppälä *et al.*, 1990; Trahan *et al.*, 1991). Although it is true that xylitol does not cause dental caries, the inhibitory mechanism of xylitol has not been confirmed in plaque biofilm *in vivo*.

Metabolome analysis is the evaluation of biological systems for changes in endogenous metabolites through comprehensive metabolite profiling. Recently, the combination of capillary electrophoresis and time-of-flight mass spectrometry (CE-MS) has been developed for separation and quantification of metabolites of the central carbon metabolism, including the EMP pathway, the pentose-phosphate pathway, and the tricarbonic acid cycle (the TCA cycle) (Edwards *et al.*, 2006; Monton and Soga, 2007; Timischl *et al.*, 2008; Ramautar *et al.*, 2009). In a previous study, CE-MS was used to analyze the metabolome in a small amount of supragingival plaque *in vivo* (Takahashi *et al.*, 2010).

In the present study, we attempted to confirm the inhibitory mechanisms of fluoride and xylitol on the central carbon metabolism of supragingival plaque *in vivo*, by performing metabolome analysis after oral rinsing with fluoride and xylitol.

MATERIALS & METHODS

Supragingival Plaque Sampling

After informed consent was obtained, six males and one female (age, 24.6 ± 4.6 yrs) were asked to refrain from toothbrushing and to allow dental plaque to accumulate overnight. The volunteers were periodontally healthy, with 0.14 ± 0.38 decayed teeth (DT), and had not taken any antibiotics recently or currently. After confirming that the volunteers had not consumed any food for at least 2 hrs, we collected all the available supragingival plaque, using sterilized toothpicks, mainly from marginal and interproximal areas of the right or left half of the dentition. Immediately, plaque samples were weighed and mixed with 0.80 mL ice-cold methanol containing internal standards (Internal standard-1; Human Metabolome Technologies, Tsuruoka, Japan) and sonicated for 30 sec (55W, US-1R; AS ONE Corporation, Osaka, Japan). About 10 mg wet weight of plaque was collected from half of the dentition. Internal standard-1 contains methionine sulfone and camphor-10-sulfonic acid for calibration of the quantification of MS. The volunteers were asked to rinse with 10 mL of 10 mM glucose, 10 mM xylitol, or a mixture of 10 mM xylitol plus 10 mM glucose for 60 sec, and after 10 min, supragingival plaque was collected from the other half of the dentition and treated as described above. For the fluoride trial, the volunteers were asked to rinse with 10 mL sodium fluoride (225 or 900 ppm F^-) for 60 sec, and supragingival plaque was collected and treated as described above. After 10 min, the volunteers were asked again to rinse with 10 mM glucose (10 mL) for 60 sec, and after 10 min, supragingival plaque was collected and treated as described above. Each volunteer rinsed with 10 mM glucose, 10 mM xylitol, 10 mM xylitol plus 10 mM glucose solution, 225 ppm NaF, and 900 ppm NaF only once with an interval of 1 wk.

The plaque samples were mixed with 0.80 mL chloroform and 0.32 mL Milli-Q water by being vortexed for 30 sec and were then centrifuged. The aqueous layer was ultrafiltrated (Ultrafree-MC 5000NMWL UFC3 LCCNB; Millipore, Billerica, MA, USA), dried for 6 to 9 hrs, suspended in Milli-Q water containing internal standards (Internal standard-3; Human Metabolome Technologies), and stored at –80°C until analysis. Internal standard-3 contains trimesic acid and 3-hydroxynaphthalene-2,7-disulfonic acid for calibration of the retention time for CE.

CE-MS Conditions

CE-MS was performed by capillary electrophoresis (G1600AX; Agilent Technologies, Waldbronn, Germany) with time-of-flight mass spectrometry (G1969A; Agilent Technologies), as described previously (Takahashi *et al.*, 2010). A fused silica capillary (H3305-2002), sheath liquid (H3301-1020), and electrolytes (H3302-1021) were used for analysis (Human Metabolome Technologies). The applied voltage was set at +30 kV, electrospray ionization was operated in the negative ion mode, and the capillary voltage was set at 3.5 kV. The flow rate of heated dry nitrogen gas (300°C) was monitored at 7 L/min. All standard metabolites and chemicals used were of analytical or reagent grade. The quantitative error of the CE-MS was less than 10%.

We analyzed data by calculating software (MassHunter WorkStation Software Qualitative Analysis; Agilent Technologies) using data obtained from standard metabolite solutions. All metabolites included in the central carbon metabolism were identified and quantified, except glyceraldehyde 3-phosphate, 2-phosphoglycerate (the EMP pathway), xylulose 5-phosphate (the pentose-phosphate pathway), and X5P, whose standards were not available. Lactate was also quantified, while acetate and formate were not quantified, because their mass-to-charge ratio (m/z) values are too small for the CE-MS.

X5P Quantification

X5P was synthesized from xylitol by enzymatic reaction of a phosphoenolpyruvate:fructose phosphotransferase system, with toluene-permeabilized cells of *S. mutans*. *S. mutans* NCTC 10449 was grown in complex media containing 1.7% tryptone, 0.3% yeast extract, and 0.5% glucose at pH 7 and 37°C under anaerobic conditions (10% H_2, 10% CO_2, 80% N_2). The cells were harvested by centrifugation, washed twice with PPB solution (2 mM potassium phosphate buffer [pH 7.0] containing 150 mM KCl and 5 mM $MgCl_2$), and stored as pellets at –20°C until use. The cell pellets were thawed, suspended in PPB solution at an optical density of 1 at 660 nm, and vortexed with 0.01 vol of toluene for 1 min. After centrifugation, the cells were suspended in the same buffer. The reaction mixture for X5P synthesis contained 60 mM xylitol, 1 mM phosphoenolpyruvate, 0.1 mM NADH, 11 U/mL lactate dehydrogenase, and the cells in PPB solution. The reaction was started with the addition of xylitol, and the decrease in NADH, which corresponds to the amount of X5P produced, was monitored photometrically at 340 nm and 37°C for 10 to 20 min. The concentration of X5P was determined by photometric calculation with the mM extinction coefficient of NADH. The photometric decrease at 340 nm was corrected by NADH oxidase activity, which oxidized NADH to NAD independently of the phosphoenolpyruvate: fructose phosphotransferase system. The reaction was terminated by the addition of 0.1 vol of 6.6 N perchloric acid and kept at 4°C overnight. The perchloric acid mixture was neutralized with 5 M potassium carbonate and used as a standard of X5P for CE-MS analysis. X5P was identified by CE-MS mass signal (m/z value) estimated from the structure formula of X5P, and was confirmed by a decrease in the signal of X5P after incubation with alkaline phosphatase, which converts X5P to xylitol.

Statistical Analysis

Differences in the amounts of metabolites between resting plaque and plaque collected after the rinses were evaluated by the paired *t* test. P-value was adjusted from 0.05 to 0.002 based on the Bonferroni correction for multiple comparisons. Differences in the amounts of lactate were also evaluated by the paired *t* test. P-value was adjusted from 0.05 to 0.017.

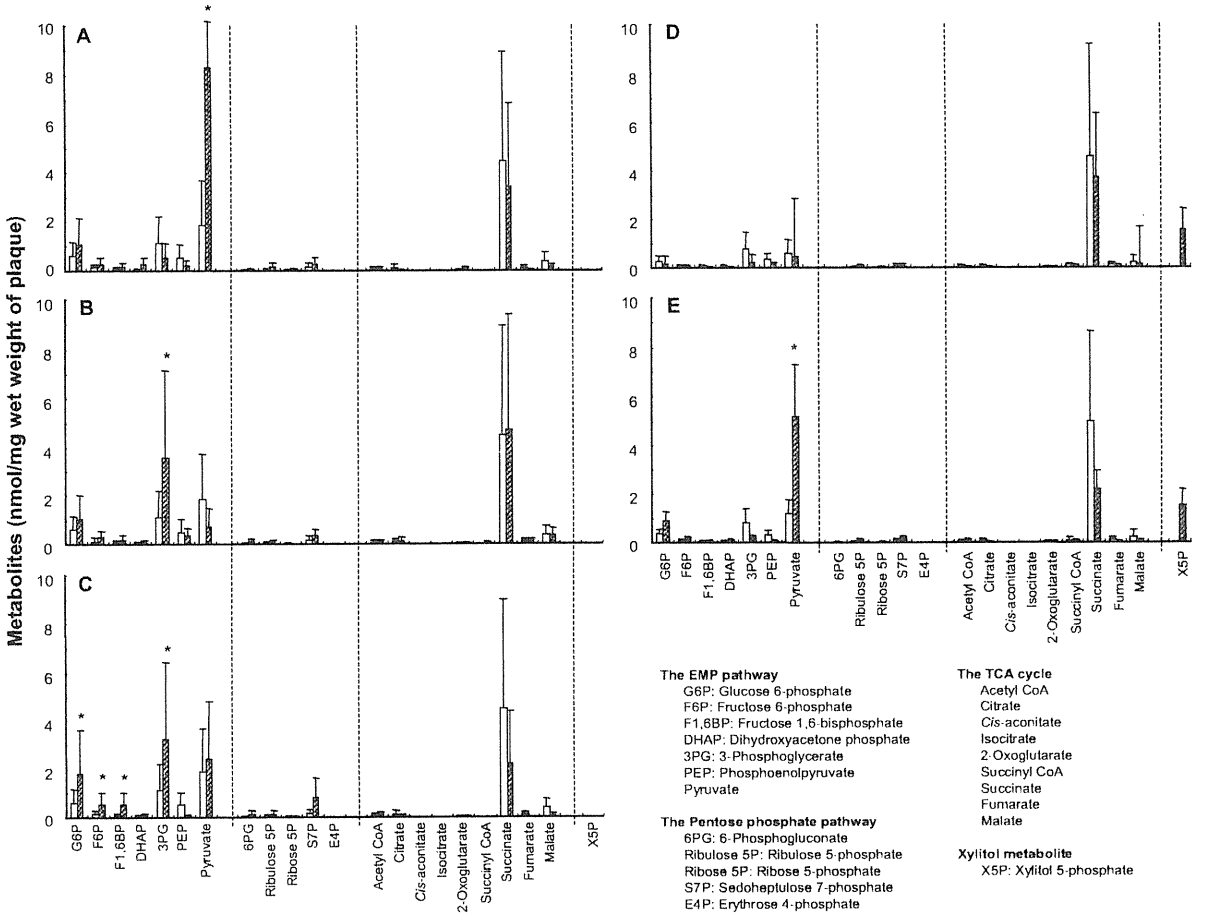

Figure 1. Effects of fluoride and xylitol on metabolome profile of supragingival plaque. **(A)** Glucose rinse (hatched box) and resting plaque (open box); **(B)** fluoride rinse (950 ppm F^-) (hatched box) and resting plaque (open box); **(C)** fluoride-glucose rinse (hatched box) and resting plaque (open box); **(D)** xylitol rinse (hatched box) and resting plaque (open box); and **(E)** xylitol-glucose rinse (hatched box) and resting plaque (open box). Values are the mean of seven individuals. Vertical bar, standard deviation. Significant difference from resting plaque (*$p < 0.002$).

RESULTS

Effects of Fluoride and Xylitol on Metabolome Profile and Lactate Production in Supragingival Plaque

In the resting supragingival plaque, most metabolites in the central carbon metabolism were detected, except for erythrose 4-phosphate in the pentose phosphate pathway and *cis*-acconitate and isocitrate in the TCA cycle (Fig. 1A). After the glucose rinse, pyruvate in the EMP pathway increased significantly. Glucose 6-phosphate increased, and 3-phosphoglycerate and phosphoenolpyruvate decreased, although these changes were insignificant. After the fluoride rinse, 3-phosphoglycerate in the EMP pathway increased significantly (Fig. 1B). Glucose 6-phosphate increased, while phosphoenolpyruvate and pyruvate decreased, although these changes were significant. After the glucose rinse after fluoride application, glucose 6-phosphate, fructose 6-phosphate, fructose 1,6-bisphosphate, and 3-phosphoglycerate in the EMP pathway were increased significantly (Fig. 1C). The metabolome profile after the xylitol rinse was similar to that of resting plaque except for the detection of X5P (Fig. 1D), while the metabolome profile after the rinse with the xylitol-glucose mixture was similar to that after the glucose rinse except for the detection of X5P (Fig. 1E).

Lactate was produced after the glucose rinse, regardless of the presence of xylitol, while lactate production was repressed significantly by the fluoride rinse prior to glucose in a dose-dependent manner (Table). The xylitol rinse did not increase lactate, which was similar to that in the resting plaque.

Changes in Metabolome Profile in the Presence of Fluoride and Xylitol

Ratios of metabolite amounts after the glucose rinse with fluoride application or the xylitol-glucose rinse to metabolite amounts after the glucose rinse (Fig. 2) show the changes in the metabolome profile more clearly. In the presence of fluoride, glucose 6-phosphate, fructose 6-phosphate, fructose 1,6-bisphosphate, and 3-phosphoglycerate in the EMP pathway and 6-phosphogluconate and sedoheptulose 7-phosphate in the pentose phosphate pathway increased, while dihydroxyacetone

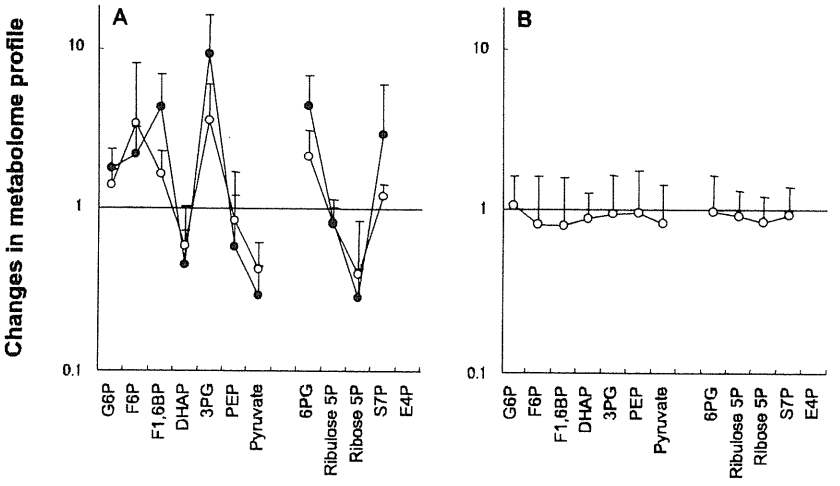

Figure 2. Changes in metabolome profile. **(A)** Fluoride-glucose rinse, 10% glucose rinse after application of fluoride containing 225 ppm F^- (open circle) or 900 ppm F^- (closed circle); and **(B)** xylitol-glucose rinse, 10% xylitol rinse with 10% glucose. The rate of change was calculated as (amount of metabolite after glucose rinse with fluoride application or xylitol-glucose rinse) / (amount of metabolite after glucose rinse). Values are the mean of seven individuals. Vertical bar, standard deviation. See Fig. 1 for abbreviations of metabolites.

Table. The Amount of Lactate in Supragingival Plaque after Glucose Rinse, Glucose Rinse with Fluoride Application, and Xylitol-Glucose Rinse

Oral Rinse Component	Lactate Concentration (nmol/mg wet weight of plaque)
Glucose	45.3 ± 21.7[a]
225 ppm Fluoride + Glucose	29.9 ± 11.6*
900 ppm Fluoride + Glucose	24.4 ± 12.5*
Xylitol + Glucose	41.1 ± 17.8
Xylitol	4.21 ± 2.90
No addition (resting plaque)	4.89 ± 6.20

[a]Mean ± standard deviation.
*Significant difference from the amount of lactate after glucose rinse ($p < 0.017$).

phosphate, phosphoenolpyruvate, and pyruvate in the EMP pathway decreased (Fig. 2A). These changes became more evident as the concentration of fluoride increased. Inhibitory steps by fluoride, expected from these results, are indicated in the metabolic pathways (Fig. 3). In contrast, there were no clear changes in the presence of xylitol (Fig. 2B). There were also no clear changes in the TCA cycle, in the presence of either fluoride or xylitol (data not shown).

DISCUSSION

The glucose rinse resulted in lactate production in supragingival plaque, with an increase of metabolites upstream and a decrease of metabolites downstream (except pyruvate) of the EMP pathway (Fig. 1A), as reported previously (Takahashi *et al.*, 2010).

The fluoride-glucose rinse promoted the intracellular accumulation of 3-phosphoglycerate (Fig. 1C) along with decreased lactate production (Table), and the amount of 3-phosphoglycerate was higher than that after the glucose rinse (Fig. 2A). These observations indicate the existence of an inhibitory step at enolase *in vivo*, which catalyzes the conversion of 2-phosphoglycerate to phosphoenolpyruvate [(1) in Fig. 3], as reported *in vitro* in *Streptococcus mutans* and *Streptococcus sanguinis* (Hata *et al.*, 1990; Maehara *et al.*, 2005). In addition, the oral rinse with only fluoride resulted in a similar metabolome profile, except for pyruvate (Fig. 1B). This suggests that supragingival plaque metabolized carbohydrates derived from saliva and bacteria-stored polysaccharides slowly and constantly, and that fluoride inhibited the metabolism and subsequently provided a metabolome profile similar to that after the fluoride-glucose rinse (Fig. 1C). This inhibition by fluoride on the glycolysis may repress bacterial growth over the long term.

In the presence of fluoride, an increase in glucose 6-phosphate, fructose 6-phosphate, and fructose 1,6-bisphosphate and a slight decrease in dihydroxyacetone phosphate were observed (Fig. 2A), suggesting the inhibition of aldolase, glyceraldehyde 3-phosphate dehydrogenase, and/or phosphoglycerate kinase in the EMP pathway [(2)-(4) in Fig. 3], although there is no report on this type of inhibition in *Streptococcus mutans* and *Streptococcus sanguinis* (Hata *et al.*, 1990; Maehara *et al.*, 2005). Further study is needed to clarify this phenomenon by investigating other plaque bacteria. The increase in 6-phosphogluconate and the decrease in ribulose 5-phosphate and ribose 5-phosphate in the presence of fluoride (Fig. 2A) suggest the inhibition of 6-phosphogluconate dehydrogenase, an enzyme in the pentose phosphate pathway (Fig. 3), which may influence bacterial growth, because this pathway is essential to supply NADPH for fatty acid synthesis and pentose phosphates for nucleotide synthesis.

In the present study, glucose was rinsed 10 min after fluoride application, and acid production was inhibited significantly. The effectiveness of the fluoride rinse on acid production of supragingival plaque is still controversial (Giertsen *et al.*, 1999), since the preservation and release of fluoride in supragingival plaque and on the tooth surface have not been elucidated well *in vivo*. However, it is possible that fluoroapatite can release fluoride in supragingival plaque (Harper and Loesche, 1986), and a recent study revealed that fluoride is preserved in supragingival plaque, and the preservation can be enhanced by pre-rinsing with calcium ions (Vogel *et al.*, 2008), suggesting that a fluoride rinse might be more effective on acid production from supragingival plaque by pre-rinsing with calcium compounds.

Xylitol had no effect on the metabolome profile and lactate production from glucose of supragingival plaque *in vivo* (Figs. 1E, 2B, and Table). X5P was detected at a significant level only after a rinse with xylitol or a xylitol-glucose mixture, as previously reported (Assev *et al.*, 1996), supporting that X5P is produced *via* a bacterial phosphoenolpyruvate-dependent phosphotransferase system (Assev and Rölla, 1984; Trahan *et al.*, 1985; Trahan, 1995).

The decrease of 3-phosphoglycerate and phosphoenoly-pyruvate (substrates of the phosphoenolpyruvate-dependent phosphotransferase system) after the xylitol rinse (Fig. 1D) suggests the involvement of this system in X5P formation. However, the presence of X5P does not seem to influence glucose fermentation by supragingival plaque *in vivo*. This might be because dental plaque covering the clinically healthy tooth surface contains only a small number of mutans streptococci (Bowden *et al.*, 1975; Nyvad and Killian, 1990), whose acid production and growth are inhibited by X5P. Another possibility is that X5P is not as effective *in vivo* as *in vitro*. Thus, it seems that the role of xylitol in caries prevention is as a non-fermentative sugar substitute, since no lactate production from xylitol and no effect of xylitol on the metabolome profile (Fig. 1D) were observed in the present study.

The present study revealed that metabolome analyses can detect metabolic regulation in supragingival plaque *in vivo*. *In vivo* effects of fluoride on supragingival plaque sugar metabolism and acid production were basically consistent with those previously reported as *in vitro* data obtained from representative oral bacteria. However, the metabolome analyses in the present study suggest an additional inhibitory mechanism of fluoride on plaque bacteria, and that xylitol is not an inhibitor of plaque acid production but rather is a non-fermentative sugar alcohol. Metabolome analyses of plaque biofilm can be applied for monitoring the efficacy of dietary components and medicines on plaque biofilm, leading to the development of effective plaque control.

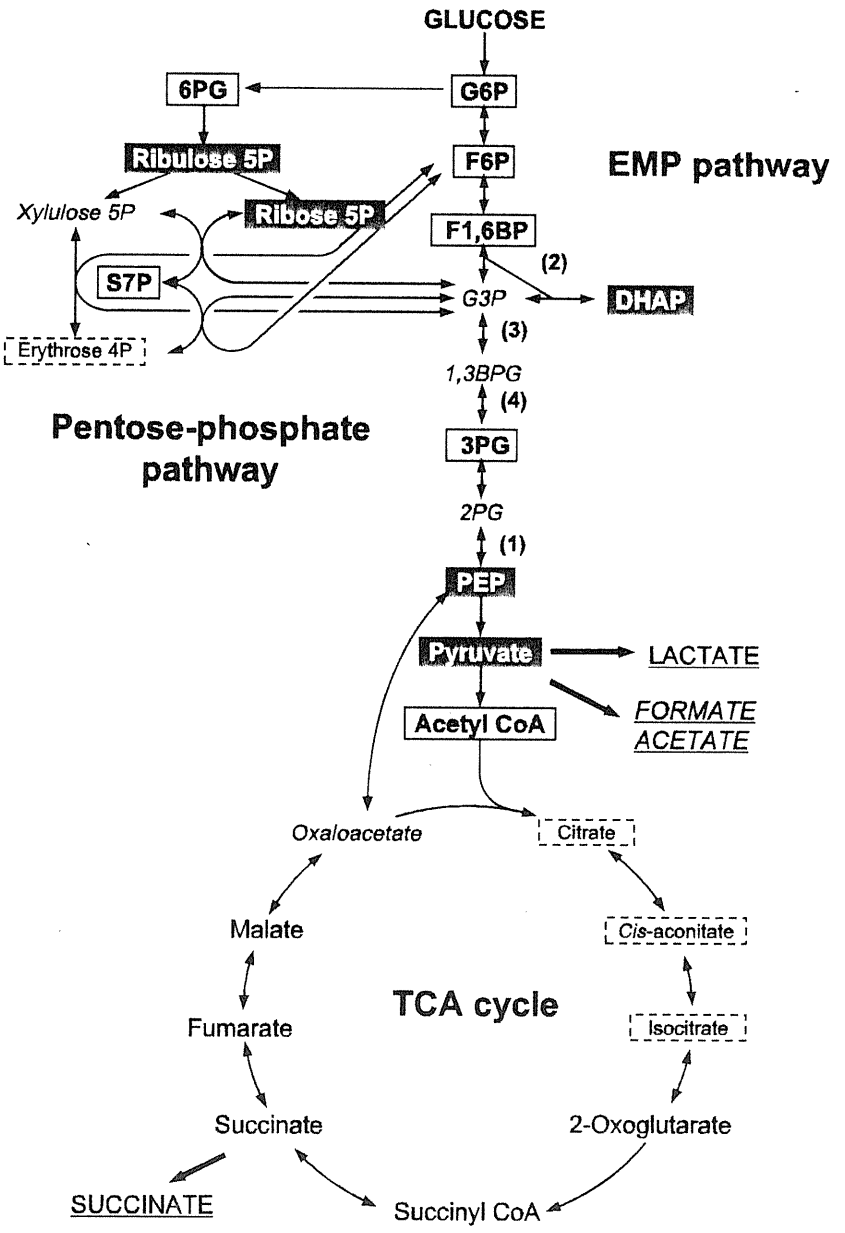

Figure 3. Expected inhibitory steps in the central carbon metabolism, including the EMP pathway, the pentose phosphate pathway, and the TCA cycle. Metabolites framed by solid lines increased in the presence of fluoride; metabolites in gray boxes decreased in the presence of fluoride; metabolites framed by broken lines showed no or low detection; and metabolites in italics were not detectable by the CE-MS system in the present study. Metabolic reactions catalyzed by (1) enolase (2PG⟷PEP), (2) aldolase (F1,6BP⟷DHAP + G3P), (3) glyceraldehyde 3-phosphate dehydrogenase (G3P⟷1,3BPG), and (4) phosphoglycerate kinase (1,3BPG,⟷,3PG). G3P, glyceraldehyde 3-phosphate; 1,3BPG, 1,3-bisphosphoglycerate; 2PG, 2-phosphoglycerate. See Fig. 1 for abbreviations of other metabolites.

ACKNOWLEDGMENTS

This study was supported by Grants-in-Aid for Scientific Research B (19390539 and 22390399), JSPS, Japan, and by Research and Education Funding for the Inter-University Research Project (2007-2011), MEXT, Japan. The authors declare no potential conflicts of interest with respect to the authorship and/or publication of this article.

REFERENCES

Assev S, Rölla G (1984). Evidence for presence of a xylitol phosphotransferase system in *Streptococcus mutans* OMZ 176. *Acta Pathol Microbiol Immunol Scand B* 92:89-92.

Assev S, Wåler SM, Rolla G (1996). Xylitol fermentation by human dental plaque. *Eur J Oral Sci* 104(Pt 1):359-362.

Bowden GH, Hardie JM, Slack GL (1975). Microbial variations in approximal dental plaque. *Caries Res* 9:253-277.

Edwards JL, Chisolm CN, Shackman JG, Kennedy RT (2006). Negative mode sheathless capillary electrophoresis electrospray ionization-mass spectrometry for metabolite analysis of prokaryotes. *J Chromatogr A* 1106:80-88.

Fejerskov O (2004). Changing paradigms in concepts on dental caries: consequences for oral health care. *Caries Res* 38:182-191.

Giertsen E, Emberland H, Scheie AA (1999). Effects of mouth rinses with xylitol and fluoride on dental plaque and saliva. *Caries Res* 33:23-31.

Guha-Chowdhury N, Clark AG, Sissons CH (1997). Inhibition of purified enolases from oral bacteria by fluoride. *Oral Microbiol Immunol* 12:91-97.

Hamilton IR (1990). Biochemical effects of fluoride on oral bacteria. *J Dent Res* 69(Spec Iss):660-667.

Harper DS, Loesche WJ (1986). Inhibition of acid production from oral bacteria by fluorapatite-derived fluoride. *J Dent Res* 65:30-33.

Hata S, Iwami Y, Kamiyama K, Yamada T (1990). Biochemical mechanisms of enhanced inhibition of fluoride on the anaerobic sugar metabolism by *Streptococcus sanguis*. *J Dent Res* 69:1244-1247.

Jenkins GN (1999). Review of fluoride research since 1959. *Arch Oral Biol* 44:985-992.

Kaufmann M, Bartholmes P (1992). Purification, characterization and inhibition by fluoride of enolase from *Streptococcus mutans* DSM 320523. *Caries Res* 26:110-116.

Maehara H, Iwami Y, Mayanagi H, Takahashi N (2005). Synergistic inhibition by combination of fluoride and xylitol on glycolysis by mutans streptococci and its biochemical mechanism. *Caries Res* 39:521-528.

Marquis RE (1990). Diminished acid tolerance of plaque bacteria caused by fluoride. *J Dent Res* 69(Spec Iss):672-675.

Miyasawa H, Iwami Y, Mayanagi H, Takahashi N (2003). Xylitol inhibition of anaerobic acid production by *Streptococcus mutans* at various pH levels. *Oral Microbiol Immunol* 18:215-219.

Monton MR, Soga T (2007). Metabolome analysis by capillary electrophoresis-mass spectrometry. *J Chromatogr A* 1168:237-246.

Nyvad B, Kilian M (1990). Comparison of the initial streptococcal microflora on dental enamel in caries-active and in caries-inactive individuals. *Caries Res* 24:267-272.

Pihlanto-Leppälä A, Söderling E, Mäkinen KK (1990). Expulsion mechanism of xylitol 5-phosphate in *Streptococcus mutans*. *Scand J Dent Res* 98:112-119.

Ramautar R, Somsen GW, de Jong GJ (2009). CE-MS in metabolomics. *Electrophoresis* 30:276-291.

Takahashi N, Washio J, Mayanagi G (2010). Metabolomics of supragingival plaque and oral bacteria. *J Dent Res* 89:1383-1388.

Tatevossian A (1990). Fluoride in dental plaque and its effects. *J Dent Res* 69(Spec Iss):645-652.

ten Cate JM (1999). Current concepts on the theories of the mechanism of action of fluoride. *Acta Odontol Scand* 57:325-329.

Timischl B, Dettmer K, Kaspar H, Thieme M, Oefner PJ (2008). Development of a quantitative, validated capillary electrophoresis-time of flight-mass spectrometry method with integrated high-confidence analyte identification for metabolomics. *Electrophoresis* 29:2203-2214.

Trahan L (1995). Xylitol: a review of its action on mutans streptococci and dental plaque—its clinical significance. *Int Dent J* 45(1 Suppl 1): 77S-92S.

Trahan L, Bareil M, Gauthier L, Vadeboncoeur C (1985). Transport and phosphorylation of xylitol by a fructose phosphotransferase system in *Streptococcus mutans*. *Caries Res* 19:53-63.

Trahan L, Néron S, Bareil M (1991). Intracellular xylitol-phosphate hydrolysis and efflux of xylitol in *Streptococcus sobrinus*. *Oral Microbiol Immunol* 6:41-50.

Vogel GL, Zhang Z, Chow LC, Schumacher GE (2002). Changes in lactate and other ions in plaque and saliva after a fluoride rinse and subsequent sucrose administration. *Caries Res* 36:44-52.

Vogel GL, Schumacher GE, Chow LC, Takagi S, Carey CM (2008). Ca prerinse greatly increases plaque and plaque fluid F. *J Dent Res* 87: 466-469.

RESEARCH REPORTS
Biomaterials & Bioengineering

G. Mayanagi[1,2], K. Igarashi[1], J. Washio[1], K. Nakajo[1], H. Domon-Tawaraya[1,3], and N. Takahashi[1]*

Evaluation of pH at the Bacteria–Dental Cement Interface

[1]Division of Oral Ecology and Biochemistry, Department of Oral Biology, Tohoku University Graduate School of Dentistry, 4-1 Seiryo-machi, Aoba-ku, Sendai, 980-8575, Japan; and [2]Research Unit for Interface Oral Health Science; and [3]Division of Pediatric Dentistry, Tohoku University Graduate School of Dentistry, Sendai, Japan; *corresponding author, nobu-t@dent.tohoku.ac.jp

J Dent Res 90(12):1446-1450, 2011

ABSTRACT

Physiochemical assessment of the parasite-biomaterial interface is essential in the development of new biomaterials. The purpose of this study was to develop a method to evaluate pH at the bacteria–dental cement interface and to demonstrate physiochemical interaction at the interface. The experimental apparatus with a well (4.0 mm in diameter and 2.0 mm deep) was made of polymethyl methacrylate with dental cement or polymethyl methacrylate (control) at the bottom. Three representative dental cements (glass-ionomer, zinc phosphate, and zinc oxide-eugenol cements) were used. Each specimen was immersed in 2 mM potassium phosphate buffer for 10 min, 24 hrs, 1 wk, or 4 wks. The well was packed with *Streptococcus mutans* NCTC 10449, and a miniature pH electrode was placed at the interface between bacterial cells and dental cement. The pH was monitored after the addition of 1% glucose, and the fluoride contained in the cells was quantified. Glass-ionomer cement inhibited the bacteria-induced pH fall significantly compared with polymethyl methacrylate (control) at the interface (10 min, 5.16 ± 0.19 *vs.* 4.50 ± 0.07; 24 hrs, 5.20 ± 0.07 *vs.* 4.59 ± 0.11; 1 wk, 5.34 ± 0.14 *vs.* 4.57 ± 0.11; and 4 wks, 4.95 ± 0.27 *vs.* 4.40 ± 0.14), probably due to the fluoride released from the cement. This method could be useful for the assessment of pH at the parasite-biomaterial interface.

KEY WORDS: pH, ISFET pH electrode, *Streptococcus*, glass-ionomer cement, fluoride, interface.

DOI: 10.1177/0022034511423392

Received February 2, 2011; Last revision May 26, 2011; Accepted May 30, 2011

INTRODUCTION

Dental caries is mainly caused by demineralization through acid production from sugar metabolism of acidogenic bacteria in the biofilm on tooth surfaces. The lost part of the tooth is filled or crowned with biomaterials to recover the form and function of the tooth. During and after caries treatment, the interface between the sound tooth structure and restoration materials provides a niche for bacteria to adhere, and the risk of secondary caries may increase. Therefore, biomaterials for restoring the teeth are desired to regulate bacterial activity, such as bacteriostatic and anti-bacterial adhesion properties, and thus a method to assess these properties of biomaterials is essential.

The observation that the pH of dental plaque decreases within a few min after sugar intake (Igarashi *et al.*, 1981, 1990; Takahashi-Abbe *et al.*, 2001) suggests that the short-term measurement of pH at the parasite-biomaterial interface is particularly needed to evaluate the inhibitory effect on microbial acid production. However, most previous studies on dental cements, including glass-ionomer cement (GIC) and zinc oxide–eugenol cement (ZOE), showed bacterial growth-inhibitory effects by incubating target bacteria in the presence of dental cements in liquid media or on agar plates for 6 hrs to 48 hrs (Boeckh *et al.*, 2002; Vermeersch *et al.*, 2005; Marczuk-Kolada *et al.*, 2006). Persson *et al.* (2005) reported that the pH fall in dental plaque formed on an ion-releasing resin, which releases hydroxyl, fluoride, and calcium ions, was inhibited *in vivo*, when compared with the pH fall on an enamel surface. However, it was not distinguished whether the inhibition was due to the suppression of bacterial growth (plaque formation), bacterial acid production, or the alteration of microbial composition by ions released from the resin. In addition, the pH at the parasite-biomaterial interface was not directly measured, due to the methodological limitation of the microtouch pH-electrode method, which may not keep the plaque structure intact by inserting the electrode into the plaque.

An ion-sensitive field-effect transistor (ISFET) pH electrode, invented by Esashi and Matsuo (1978), is very small and highly sensitive due to low internal electric resistance, and is not cytotoxic (Esashi and Matsuo, 1978). Thus, the ISFET pH electrode enabled us to measure *in vivo* acid production by human dental plaque (Igarashi *et al.*, 1981; Chida *et al.*, 1986), and artificial fissure plaque (Igarashi *et al.*, 1989, 1990). In addition, the ISFET pH electrode is small enough to assess pH at the interface between parasites and biomaterials, and is suitable for the development of a new apparatus to assess pH at the interface *in vitro*.

The present study therefore aimed to develop a new method to evaluate pH at the bacteria–dental cement interface, using an ISFET pH electrode to verify

Table. Dental Cements Used in This Study

Dental Cements	Product Name	Manufacturer	Main Components (Batch No.)	
			Powder	Liquid
Glass-ionomer cement (GIC)	FUJI IX GP®	GC, Tokyo, Japan	Fluoroaluminosilicate glass, Polyacrylic acid, (1002091)	Polyacrylic acid, Polybasic carboxylic acid (0911111)
Zinc phosphate cement (ZPC)	Elite cement 100®	GC, Tokyo, Japan	Zinc oxide (0911021)	Phosphoric acid (0910021)
Zinc oxide-eugenol cement (ZOE)	Eugedain®	Showa Yakuhin Kako, Tokyo, Japan	Zinc oxide, Benzoic acid, Magnesium stearate (9128QA)	Clove oil, Olive oil, Rosin (9125NA)

the hypothesis that conventional dental cements for filling restoration, such as GIC and ZOE, have an inhibitory effect on pH fall by bacterial acid production from sugar metabolism, compared with zinc phosphate cement (ZPC). In addition, the amount of fluoride released from dental cement was quantified during the pH fall by bacterial acid production.

MATERIALS & METHODS

Bacterial Strain and Growth Conditions

Streptococcus mutans NCTC 10449 was pre-cultured on TYG media containing 1.7% tryptone (Becton, Dickinson and Company, Franklin Lakes, NJ, USA), 0.3% yeast extract (Becton, Dickinson and Company), 0.5% NaCl, and 0.5% glucose at pH 7.0 and 37°C under anaerobic conditions (80% N_2, 10% H_2, and 10% CO_2). The pre-cultures were then transferred to new TYG media (inoculum size, 5%) and incubated under the same conditions. When the cells reached an exponential growth phase (about 0.5 of optical density at 660 nm), they were harvested by centrifugation (21,000 × *g* for 15 min at 4°C), washed with 2 mM potassium phosphate buffer (PPB, pH 7.0), and suspended in the same buffer. Bacterial cells were incubated in air at 37°C for 1 hr to exhaust intracellularly accumulated polysaccharide, and washed with 2 mM PPB (pH 7.0). The cell suspension was distributed into 1.5 mL tubes and centrifuged (16,000 × *g* for 7 min at 4°C). The pellets were stored at 4°C until used.

Materials

Three representative dental cements, GIC, ZPC, and ZOE, were used in the present study (Table). Test disks of the studied materials were prepared with a polymethyl methacrylate plate (8.0 mm in diameter, 2.0 mm thick) as a mold according to the manufacturer's instructions. After the cement hardened, each specimen was immersed in 8 mL of 2 mM PPB at pH 7.0 in polyethylene tubes. Samples were artificially aged by being stored in a thermostatic chamber at 37°C for 10 min, 24 hrs, 1 wk, or 4 wks.

Experimental Apparatus and Measurement of pH

An experimental apparatus with a well (4.0 mm in diameter and 2.0 mm deep) for pH monitoring was made of polymethyl methacrylate with a specimen of dental cement at the bottom (Fig. 1). An ISFET pH electrode (H^+ ion-sensitive area, 2.0 mm long, 1.0 mm wide, and 0.2 mm thick; model PH-60T1; Nihon Koden, Tokyo, Japan) was placed on the cement. Cells of *S. mutans*, stored at 4°C, were packed into the well by means of a spatula and a syringe and kept at 37°C for 10 min. Then, a 500-μL quantity of 1% glucose or de-ionized water was added to the cells. The pH was monitored continuously with a pH meter (ISFET mV/pH METER, BAS, Tokyo, Japan) attached to a chart recorder (LR 4220, Yokogawa Electric Corporation, Tokyo, Japan) in an incubator (Merck KGaA, Darmstadt, Germany) at 37°C for 90 min. A polymethyl methacrylate plate (No. 99997, Sanplatec, Osaka, Japan) was used as the control material, since this material is stable physically, chemically, and biologically, and is not cytotoxic under the experimental conditions in the present study.

Measurement of Fluoride Concentration

After measurement of pH fall, the remaining glucose or de-ionized water was absorbed by filter paper, and bacterial cells were collected with a spatula and pipetted with 500 μL of 2 mM PPB into polyethylene tubes. A mixed solution of sodium acetate buffer and perchloric acid (pH 5.0) was added to the bacterial cell suspension at a final concentration of 1 M. The cell suspensions were kept at 4°C overnight for complete destruction of bacterial cells. The cell extracts were collected by centrifugation, and the fluoride concentration in the extracts was measured by a fluoride-ion-specific electrode (Model 9409 BN, Orion, Cambridge, MA, USA) and a comparison electrode (Model 900100, Orion). This measurement was based on the method of Hallsworth *et al.* (1976). The concentration of fluoride in the PPB used for cement immersion was also measured. It was confirmed that the concentration of fluoride in PPB before experiment was less than the detection level (< 0.53 μM).

Statistical Analysis

The differences in pH between control and dental cements at 90 min after glucose addition were evaluated by Dunnett's test. The differences in fluoride amounts in the *S. mutans* cells with glucose and without glucose were evaluated by paired t test. The concentrations of fluoride in the PPB used for cement immersion at different immersion times were analyzed by one-way analysis of variance (ANOVA) followed by Tukey's multiple comparison. A p value of < 0.05 was considered significant.

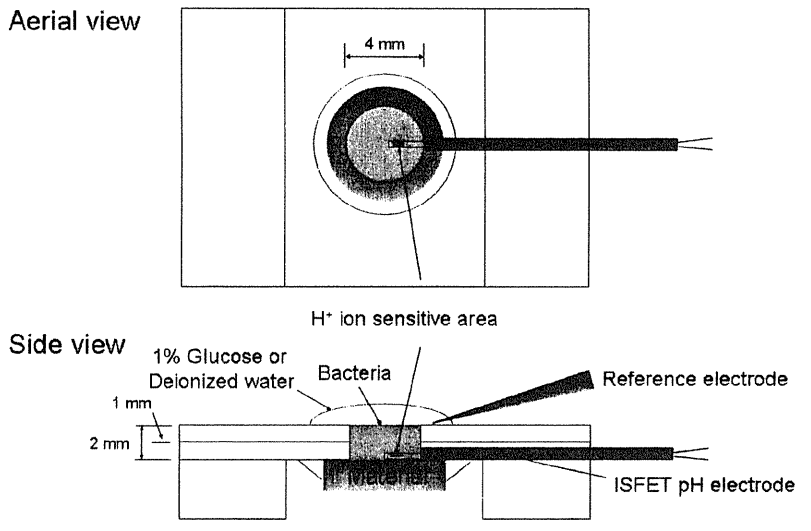

Figure 1. Schematic drawing of the experimental apparatus used in this study.

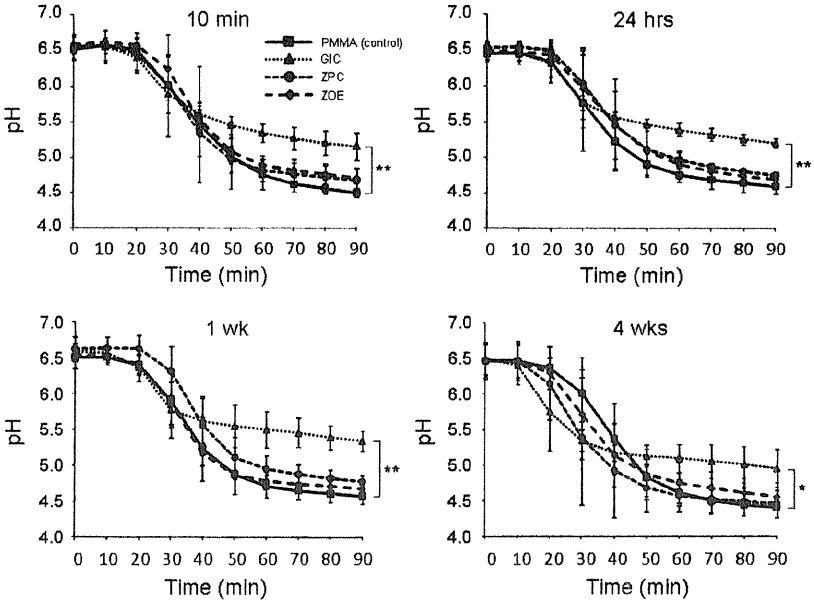

Figure 2. The pH fall curves at the interface between the cell mass of *S. mutans* NCTC 10449 and different biomaterials (3 dental cements and polymethyl methacrylate) after addition of 1% glucose. The dental cements were immersed in the buffer for 10 min, 24 hrs, 1 wk, and 4 wks. PMMA, polymethyl methacrylate; GIC, glass-ionomer cement; ZPC, zinc phosphate cement; ZOE, zinc oxide-eugenol cement. The data are the means of 3 independent experiments. Vertical bars indicate standard deviations. *$p < 0.05$, **$p < 0.01$ (significantly different from the control at 90 min after glucose addition).

RESULTS

pH Fall at the Interface

The pH fall by bacterial glucose fermentation in the presence of the materials after the addition of 1% glucose at the interface between *S. mutans* and materials is shown in Fig. 2. GIC inhibited the rate of pH fall by bacterial glucose fermentation at the interface around pH 5.5, whereas ZPC and ZOE had no inhibitory effects. The pH at the interface with GIC at 90 min was significantly higher than that with polymethyl methacrylate, regardless of the immersion time of dental cements (Fig. 2). The pH at the interface without glucose addition at 90 min was between 6.50 and 6.98 (data not shown).

Concentration of Fluoride

The amounts of fluoride contained in *S. mutans* cells at the interface with GIC after 90 min are shown in Fig. 3A. Fluoride was detected in *S. mutans* cells, regardless of the addition of glucose. However, the amounts of fluoride in *S. mutans* cells after glucose addition were significantly higher than in those without glucose addition, except at 4 wks. The amounts of fluoride in the cells on polymethyl methacrylate, ZPC, and ZOE were less than the detection level (< 0.27 nmol/well).

The fluoride contents of the immersion fluid of GIC are shown in Fig. 3B. As the immersion time was prolonged, the amounts of fluoride in the PPB increased gradually, although the increase was not significant after 24 hrs. The fluoride contents in the PPB used for cement immersion of ZPC and ZOE were less than the detection level (< 0.53 μM).

DISCUSSION

The pH at the parasite-material interface was successfully monitored by the experimental apparatus with an ISFET pH electrode. In this apparatus, the pH was stable for about 10 to 20 min after glucose addition, because it took time for glucose to diffuse into *S. mutans* cells and also for *S. mutans* to produce acids from glucose (Dawes and Dibdin, 1986; Hata and Mayanagi, 2003). When the acids penetrated the interface between *S. mutans* and cements or polymethyl methacrylate, the pH started to decrease. In contrast, the cement components were expected to diffuse into the interface gradually, affecting bacterial glucose metabolism and organic acid production. In addition, bacterial acidification probably influenced the diffusion of cement components from the corresponding cement. The pH at the interface can be determined due to these interactions between bacteria and dental cement.